

# Day 3. Reminder: Overview

## Day 1: Principles of gravitational lensing

Brief history of gravitational lensing

Light deflection in an inhomogeneous Universe

Convergence, shear, and ellipticity

Projected power spectrum

Real-space shear correlations

## Day 2: Measurement of weak lensing

Galaxy shape measurement

PSF correction

Photometric redshifts

Estimating shear statistics

## Day 3: Surveys and cosmology

Cosmological modelling

Results from past and ongoing surveys (CFHTlenS, KiDS, DES)

Euclid

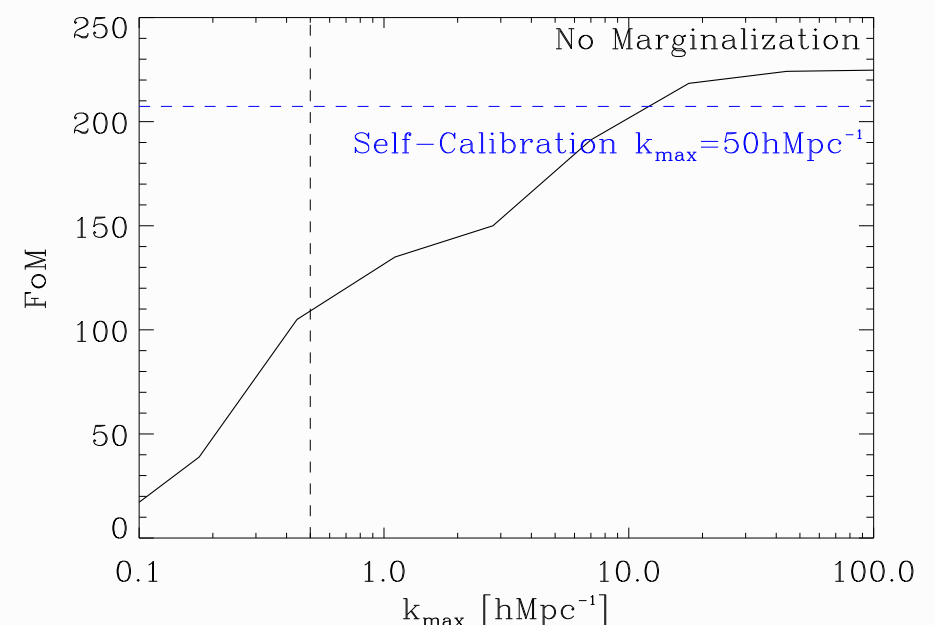
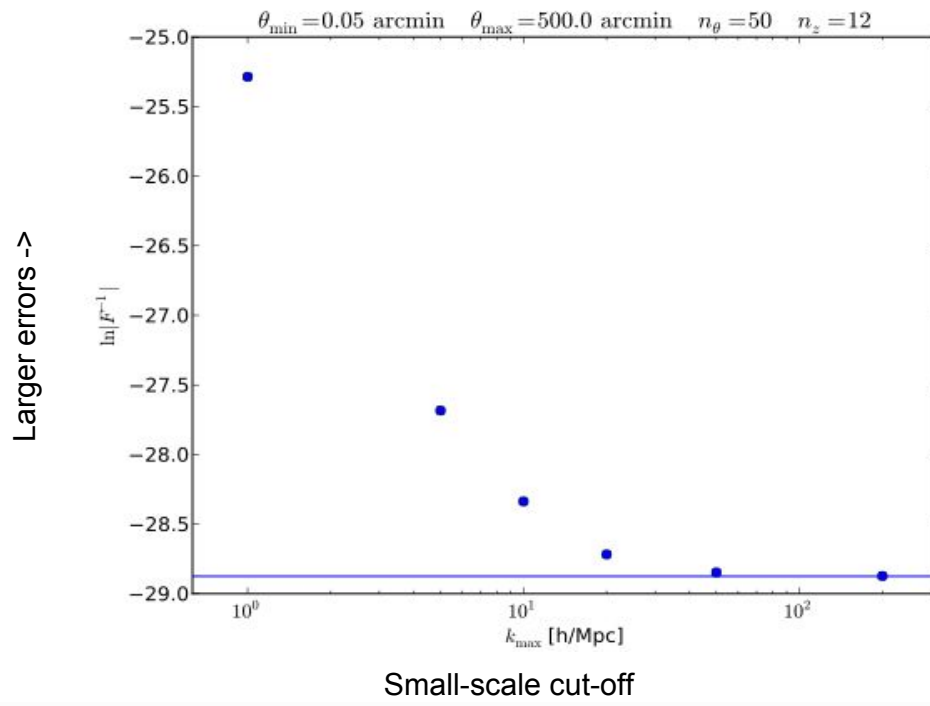
## Day 3+: Extra stuff

### Exercises

Python programming

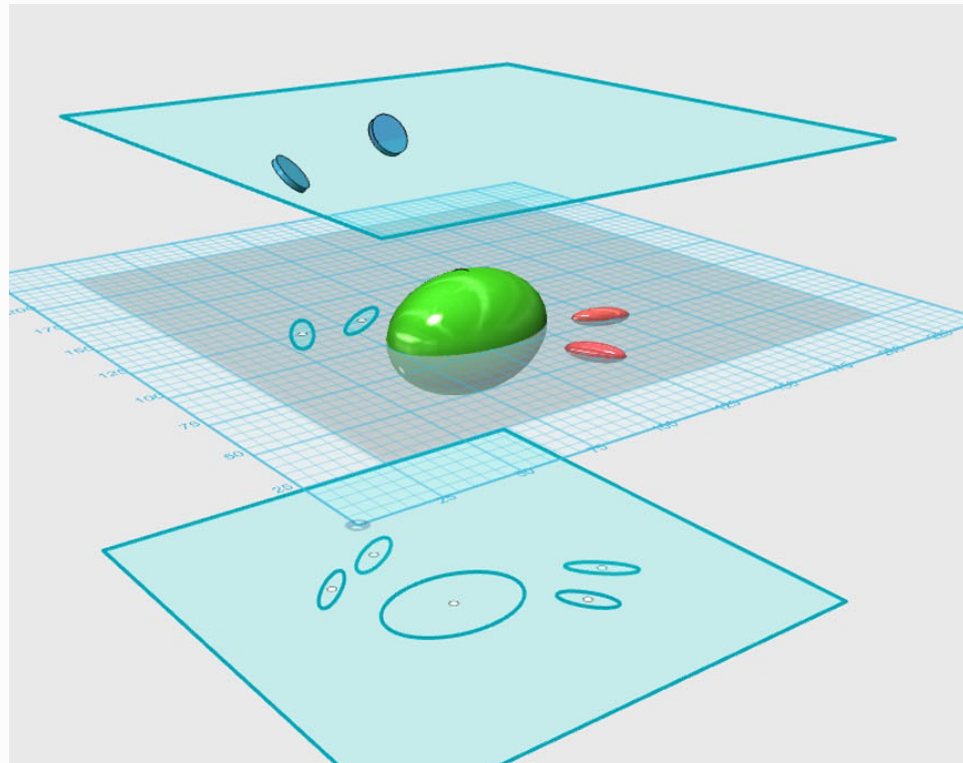
Calculations

# Non-linear modeling of the LSS



(Kitching & Taylor 2011)

# Intrinsic galaxy alignment (IA)



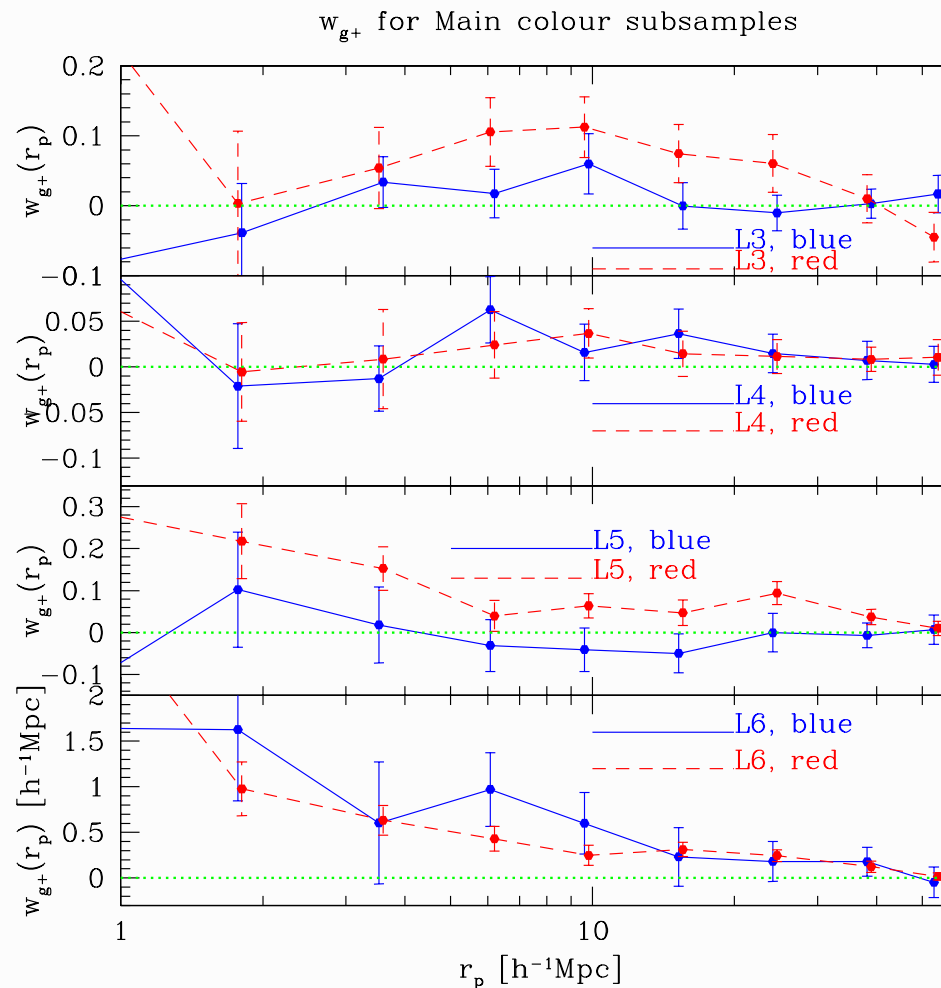
(Joachimi et al. 2015)

Contamination to cosmic shear at  $\sim 1 - 10\%$ .  
Need to model galaxy formation.

Galaxy shapes are correlated with surrounding tidal density field, due to coupling of spins for spiral galaxies, tidal stretching for elliptical galaxies. Shape of galaxies is sum of shear ( $G$ ) and intrinsic ( $I$ ) shape (remember  $\varepsilon \approx \varepsilon^s + \gamma$ ). So, with intrinsic alignment, the correlation of galaxy shapes is not only shear-shear ( $GG$ ), but also intrinsic-intrinsic ( $II$ ) and shear-intrinsic ( $GI$ ; (Hirata & Seljak 2004)).

# IA measurement: Ellipticity - density correlations

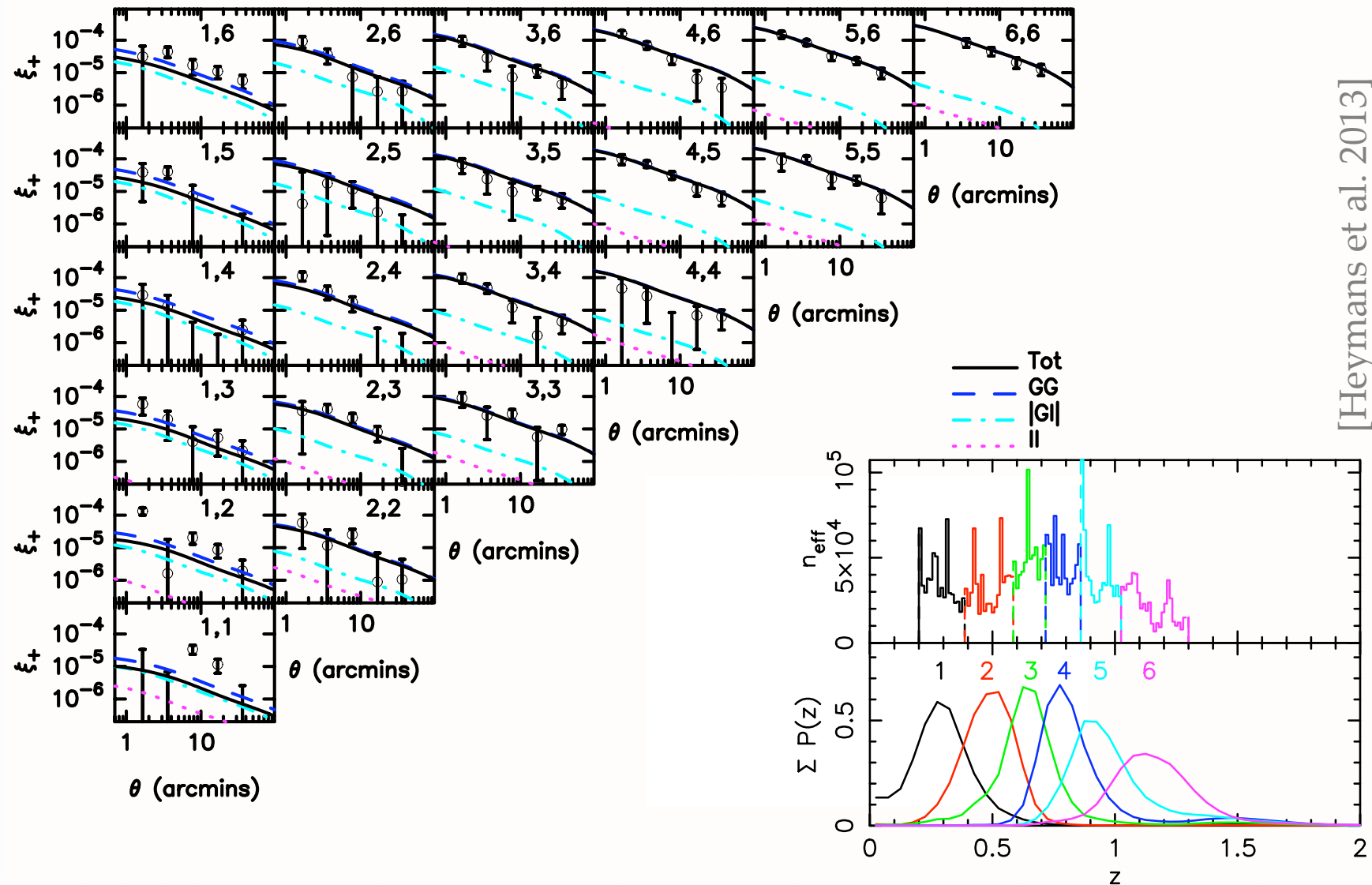
With (spectroscopic) data measure  $\gamma_t$  around massive galaxies (= centres of halos): shape - density correlations.



(Hirata et al. 2007)  
[Weak] Gravitational Lensing

# IA measurement: Ellipticity - ellipticity correlations

With photometric data measure sum of GG, GI, and II.



[Heymans et al. 2013]

# IA constraints

Simple intrinsic alignment model:

Galaxy ellipticity linearly related to tidal field

[Hirata & Seljak 2004, Bridle & King 2007].

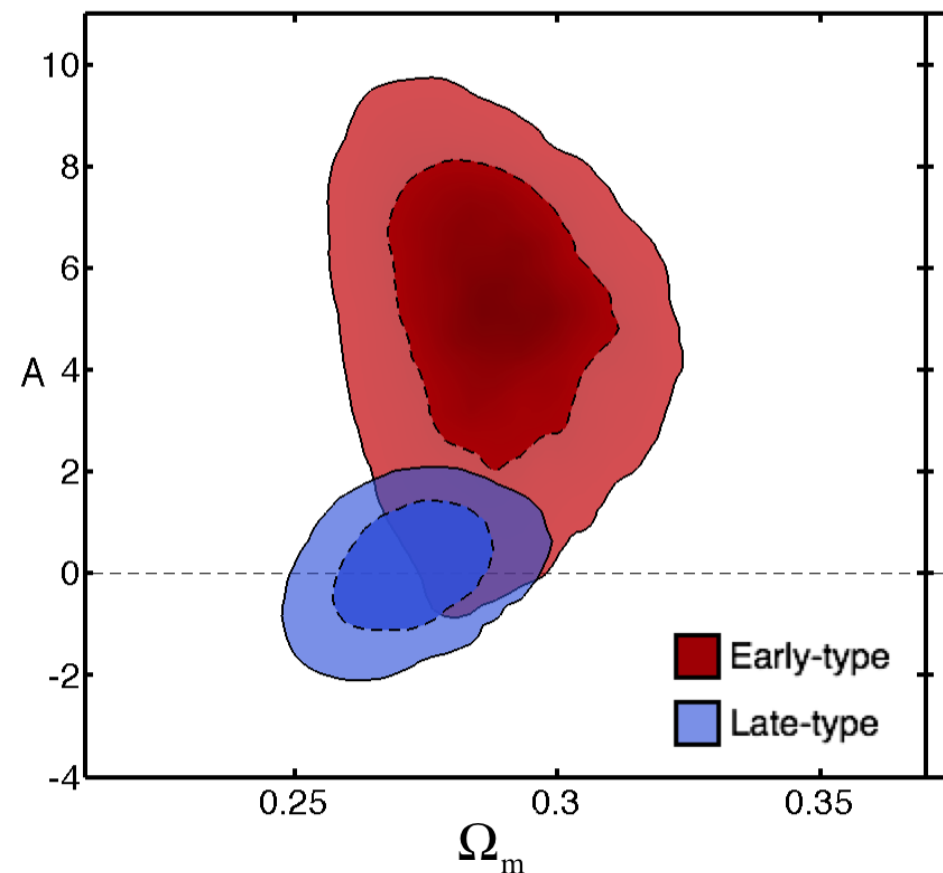
One free amplitude parameter  $A$ ,  
fixed  $z$ -dependence.

$A = 1$ : reference IA model.

$A = 0$ : no IA

$$A_{\text{late}} = 0.18^{+0.83}_{-0.82}$$

$$A_{\text{early}} = 5.15^{+1.74}_{-2.32}$$

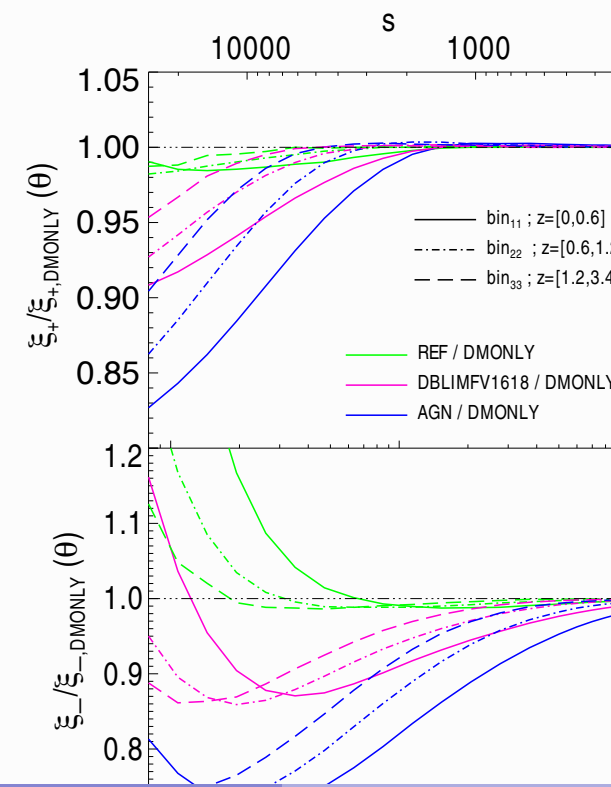
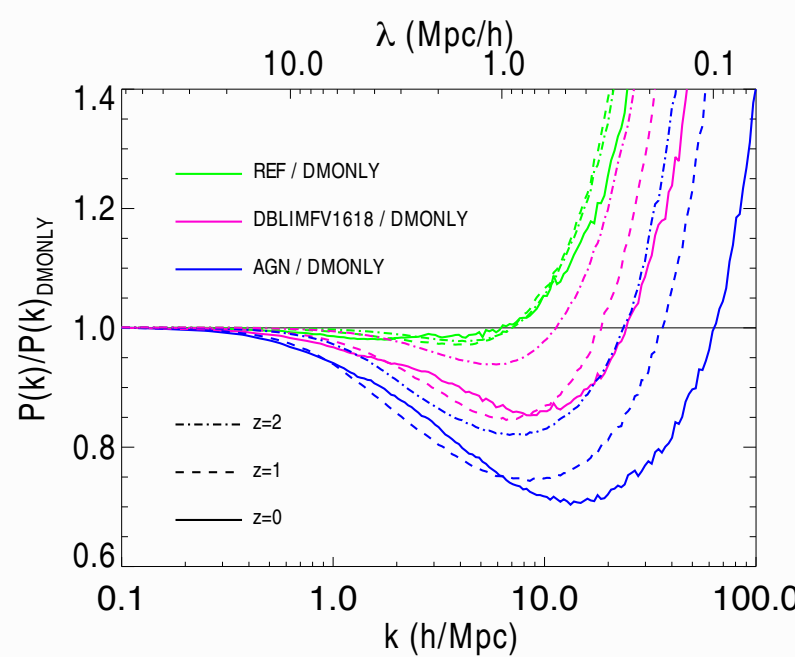


[Heymans et al. 2013]

# Baryons in the LSS

On small (halo) scales, dark-matter only models do not correctly reproduce clustering:

- $R \sim 1 - 0.1$  Mpc: gas pressure  $\rightarrow$  suppression of structure formation, gas distribution more diffuse wrt dm
- $R < 0.1$  Mpc ( $k > 10/\text{Mpc}$ ): Baryonic cooling, AGN+SN feedback  $\rightarrow$  condensation of baryons to form stars and galaxies, increase of density, stronger clustering



# CFHTLS/CFHTlenS

Groundbreaking for weak cosmological lensing:

- MegaCam 1 deg<sup>2</sup> fov (@ 3.6m CFHT)
- Multiple optical bands → photometric redshifts, tomography
- Large team (> 20; led by Yannick Mellier, Catherine Heymans, Ludovic van Waerbeke), thorough testing, multiple pipelines
- Public release of all data and lensing catalogues ([www.cfhtlens.org](http://www.cfhtlens.org))



# Canada-France-Hawaii Telescope Legacy Survey: Canada-France collaboration

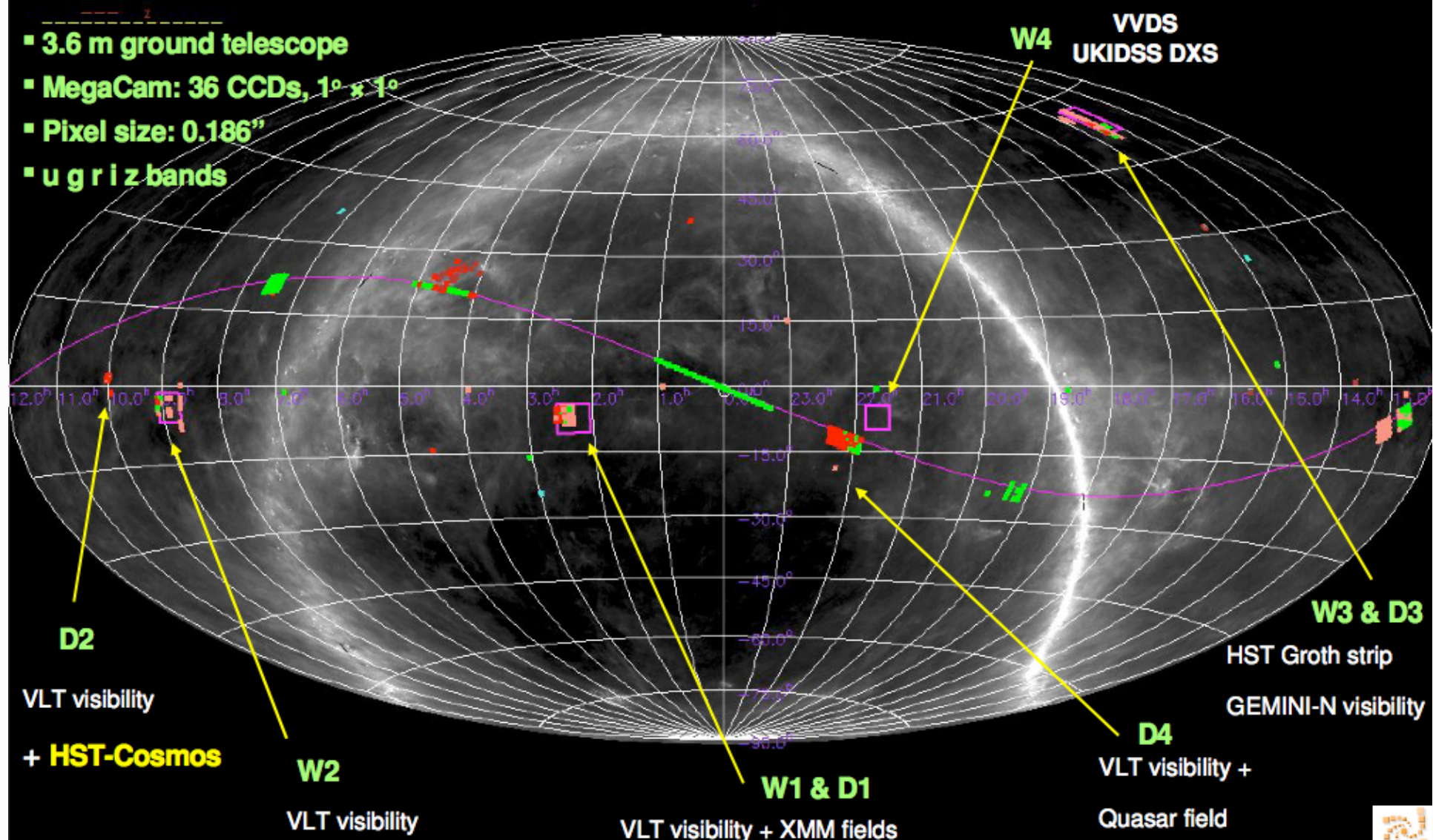
- 500 nights between June 2003 and June 2008
- 4 CFHTLS-Wide ( 170 deg<sup>2</sup> ), 4 CFHTLS-Deep ( 1 deg<sup>2</sup> each )

- 3.6 m ground telescope

- MegaCam: 36 CCDs, 1° x 1°

- Pixel size: 0.186"

- u g r i z bands

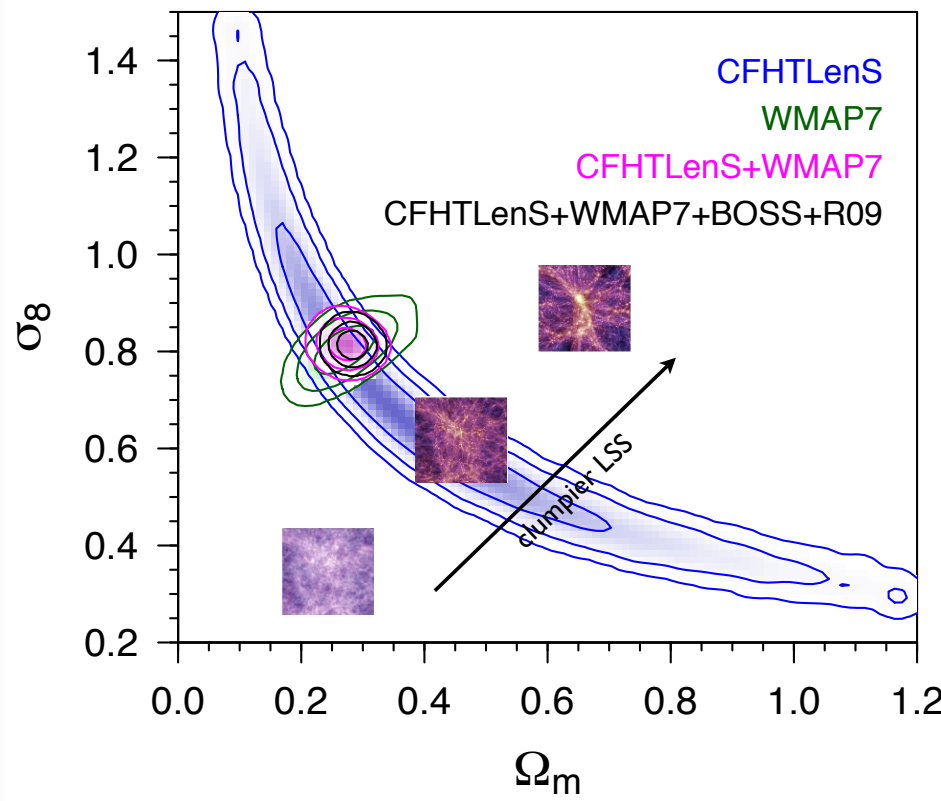


Terapix/Skywatcher : all data 03A-05A : 20000 Megacam images

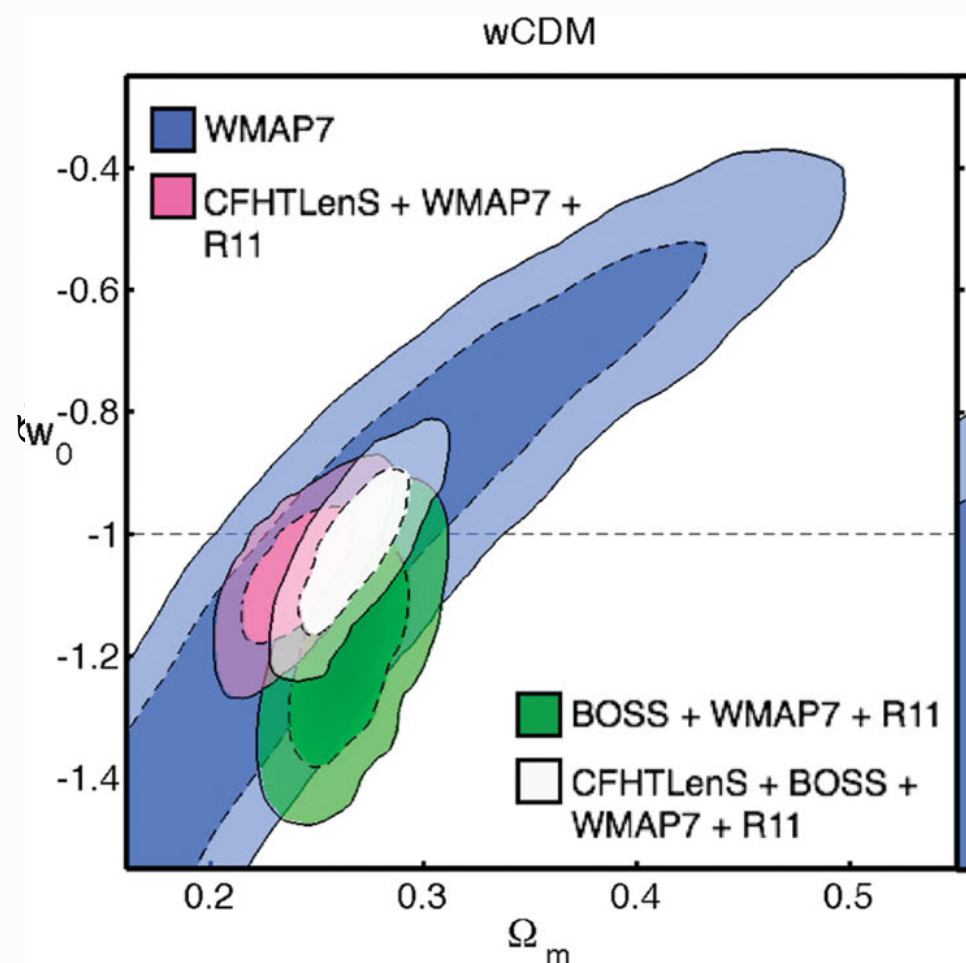
← command line : skywatcher



# CFHTlenS cosmological constraints



2D lensing  
(Kilbinger et al. 2013)



6-bin tomography  
(Heymans et al. 2013)

# CFHTLenS modified gravity

$$ds^2 = -(1 + 2\varphi)dt^2 + (1 - 2\phi)a^2dx^2$$

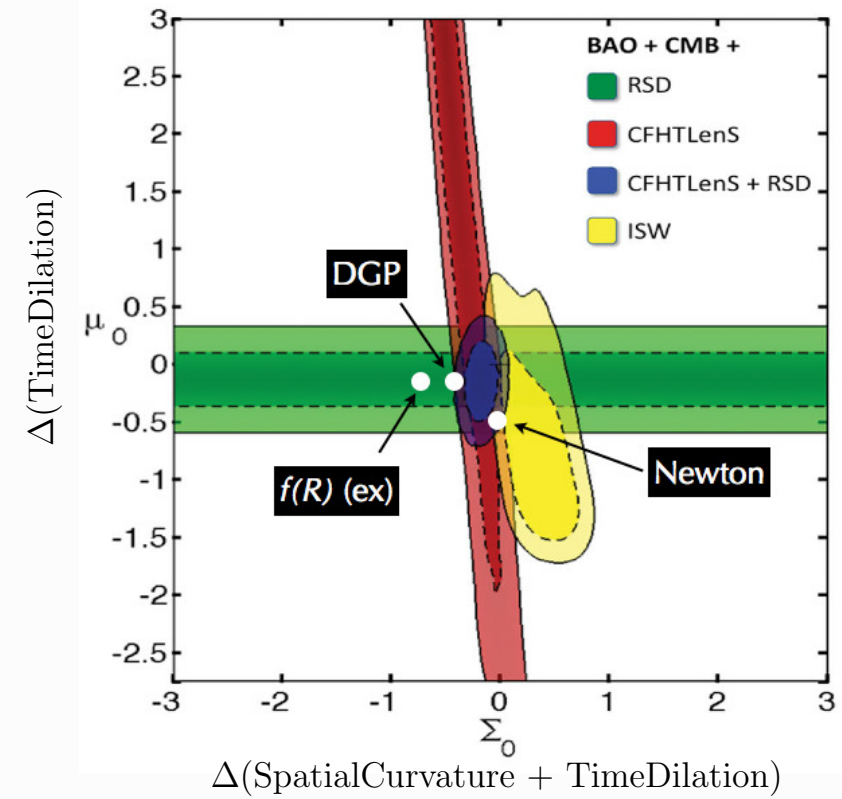
time dilation      spatial curvature

■ Gravitational potential as experienced by galaxies:

$$\nabla^2\varphi = 4\pi G a^2 \bar{\rho} \delta [1 + \mu] \quad \mu(a) \propto \Omega_\Lambda(a)$$

■ Gravitational potential as experienced by photons:

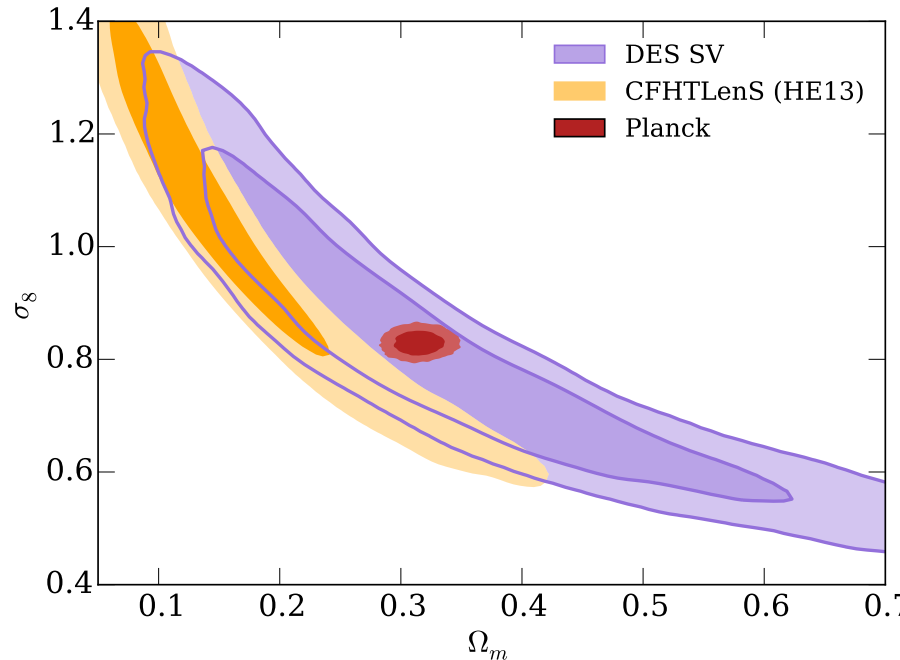
$$\nabla^2(\varphi + \phi) = 8\pi G a^2 \bar{\rho} \delta [1 + \Sigma] \quad \Sigma(a) \propto \Omega_\Lambda(a)$$



2-bin tomography  
(Simpson et al. 2013)

# DES — Dark Energy Survey

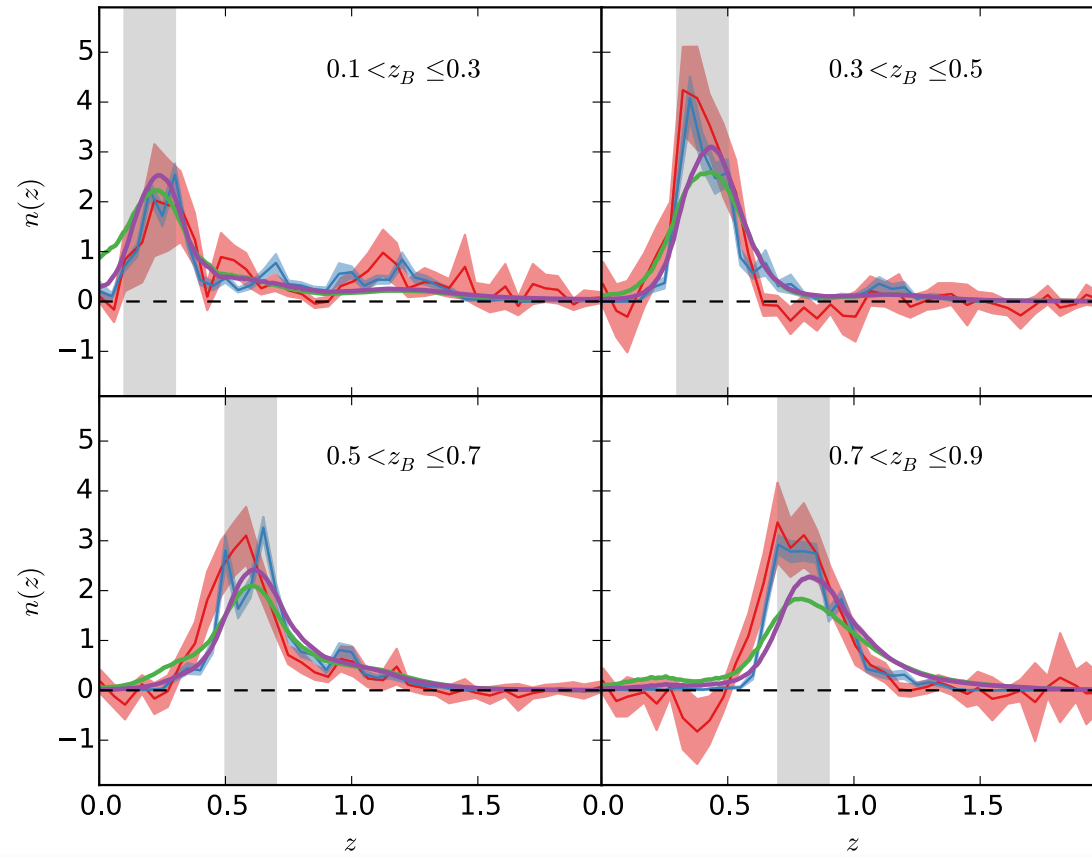
- Dedicated new camera: DECam, 3 deg<sup>2</sup> fov, weak lensing as main science goal
- @ 4m class Blanco telescope on Cerro Tololo, Chile
- 5,000 deg<sup>2</sup> when completed
- Large coverage in other wavelength (e.g. SPT)
- Ongoing survey, published results (2016) from Science Verification Data, 139 deg<sup>2</sup> = 3% of final area, but nominal depth and filters



(The Dark Energy Survey Collaboration et al. 2016)

# KiDS

- 1,500 deg<sup>2</sup> in four optical (+ 5 IR) bands
- New camera (OmegaCAM 1 deg<sup>2</sup> fov) and telescope (2.6 m VST), long delay
- Compared four different redshift estimation methods



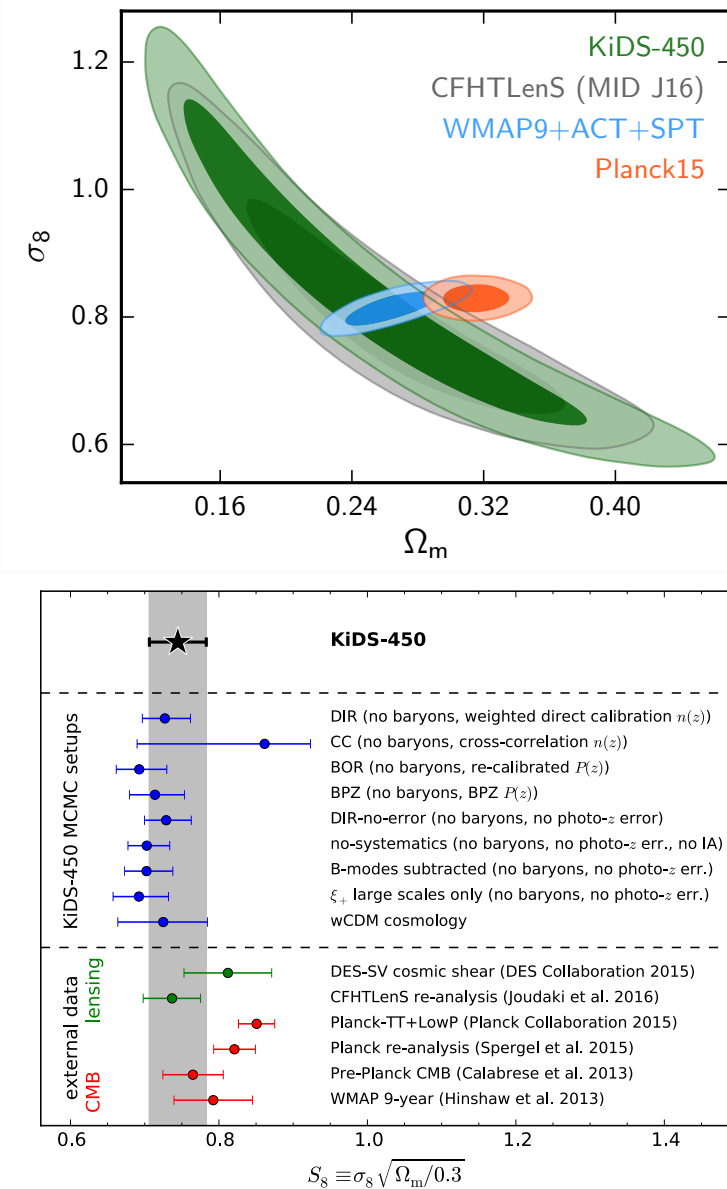
(Hildebrandt et al. 2016)

# KiDS

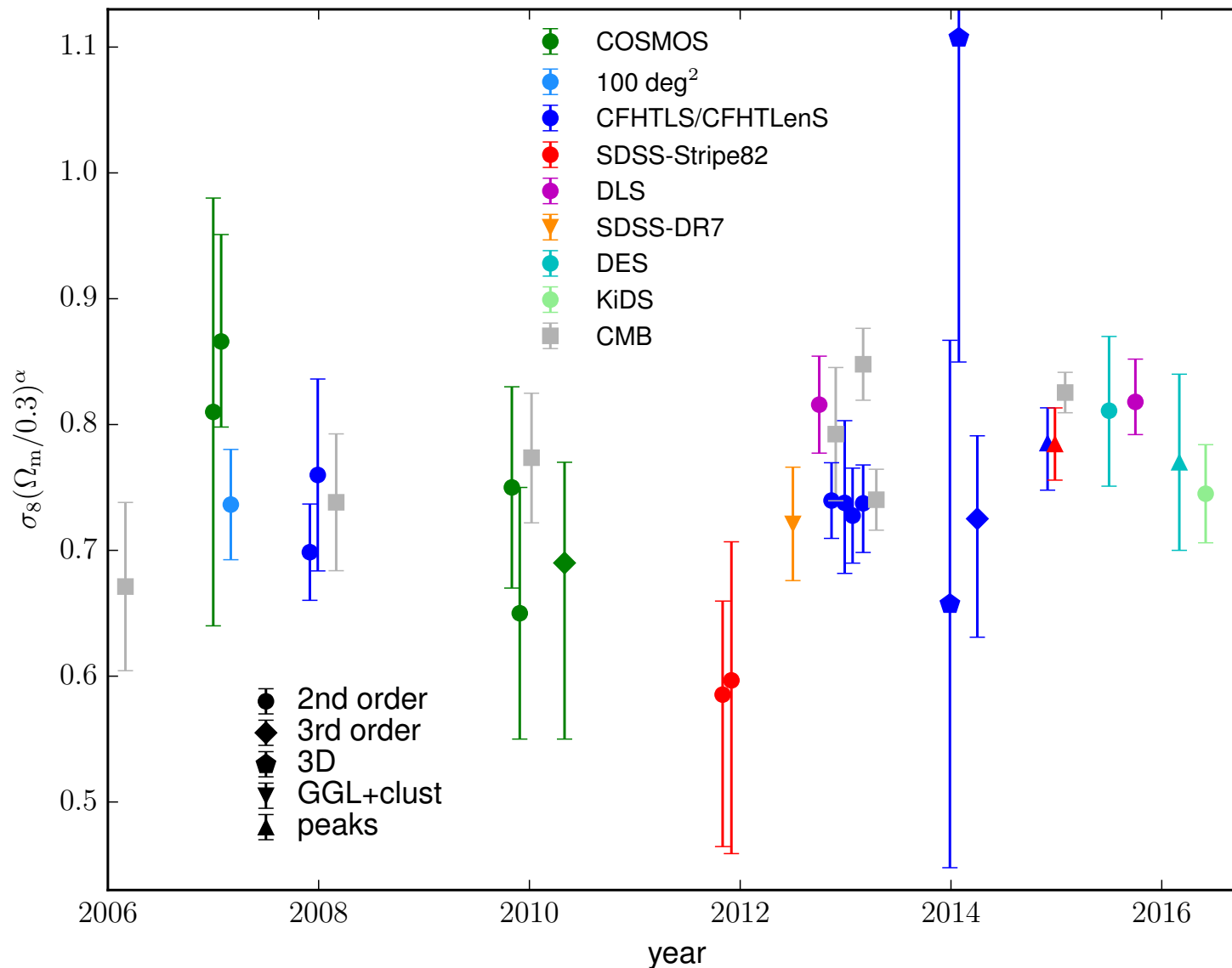
Very thorough weak-lensing analysis, including:

- $n(z)$  errors
- IA, baryonic effects
- Shear calibration
- Non-Gaussian covariance
- Blinded analysis

(Hildebrandt et al. 2016)



# Summary



# Discrepancy with Planck?

- Maybe not ( $2 - 3\sigma$ ). However, also discrepancy of CMB  $C_\ell$ 's with SZ cluster counts.
- Additional physics, e.g. massive neutrinos? Not sufficient evidence.
- WL systematics? (E.g. shear bias, baryonic uncertainty on small scales.) KiDS say not likely.

# The Euclid mission

Why is Euclid so special and challenging?

Increase of factor **100** in data volume compare to current surveys!

Few Million to few 100 Million galaxies.

For 2PCF: Naive increase of  $n_{\text{correl}}$  by 10,000!

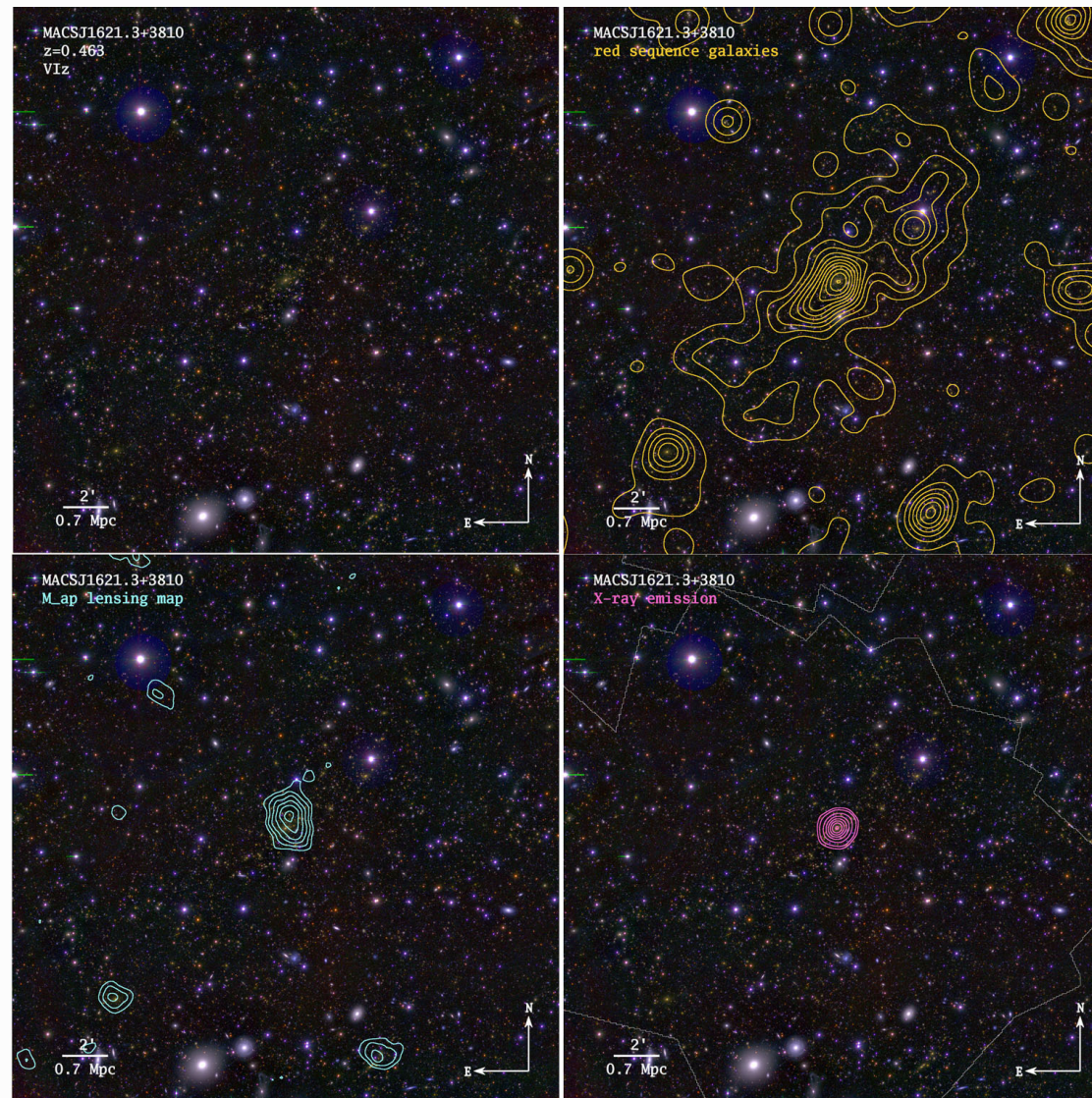
Comparison with Planck:

Planck all-sky, pixel size  $\sim 7$  arc min.

Euclid 1/3 sky, pixel size  $\sim$  typical angular distance between galaxies  $\sim$  arc sec.

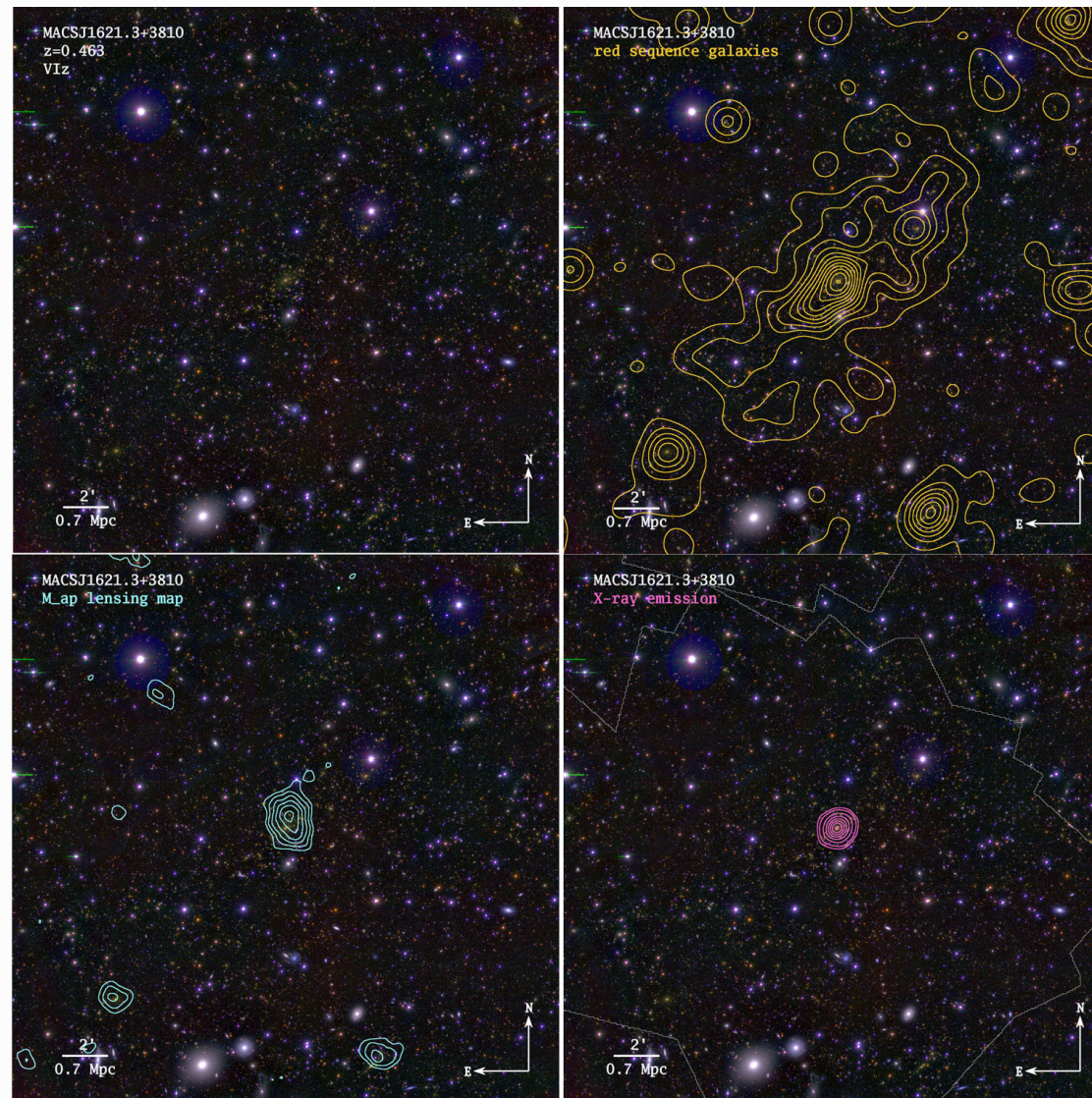
Factor  $10^5$  more pixels!

# Weak-lensing resolution



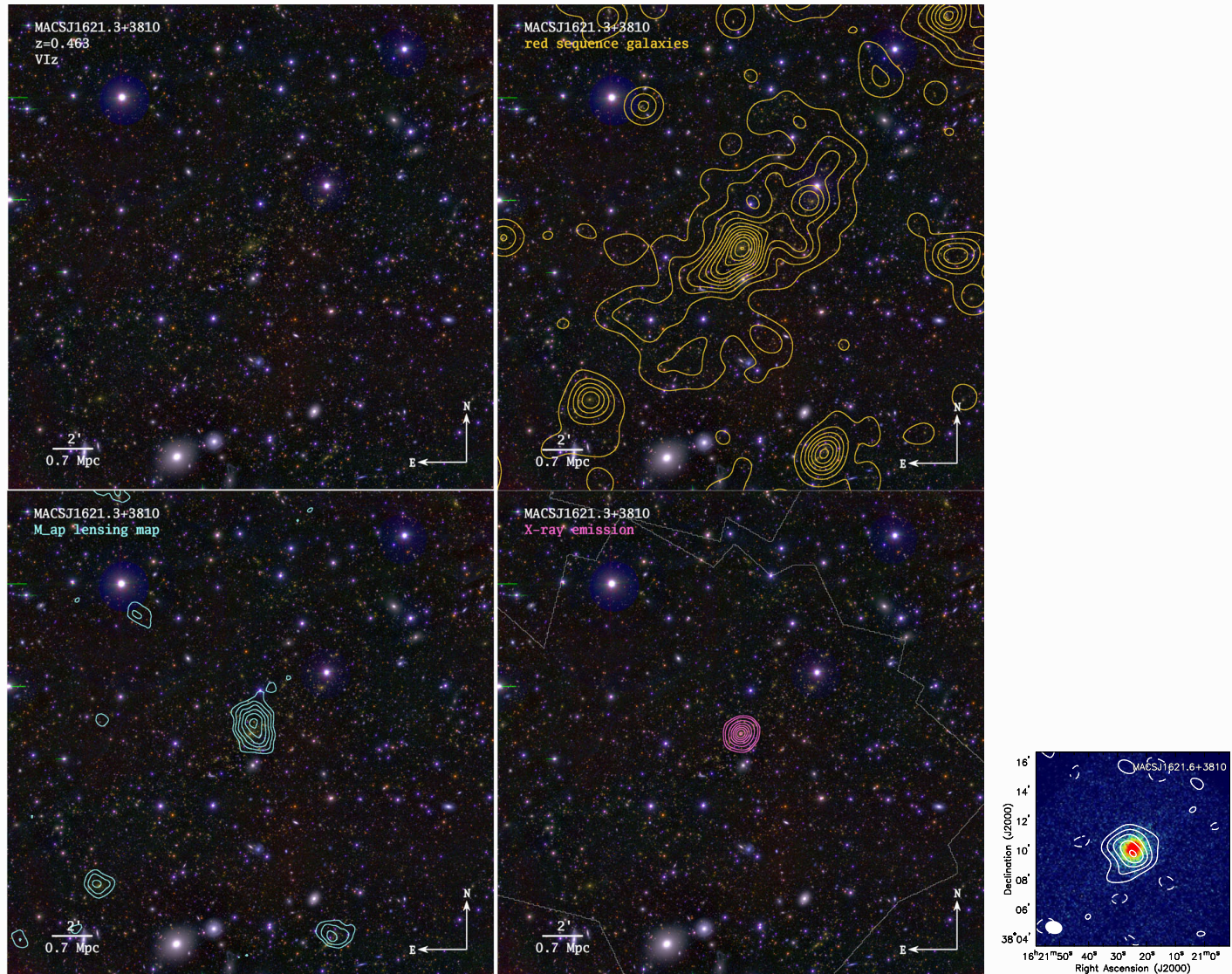
(von der Linden et al. 2014) — MACS\_J1621+3810, ground-based data,  
 $n_{\text{gal}} = 2.5 \dots 25 \text{ arcmin}^{-2}$

# Weak-lensing resolution



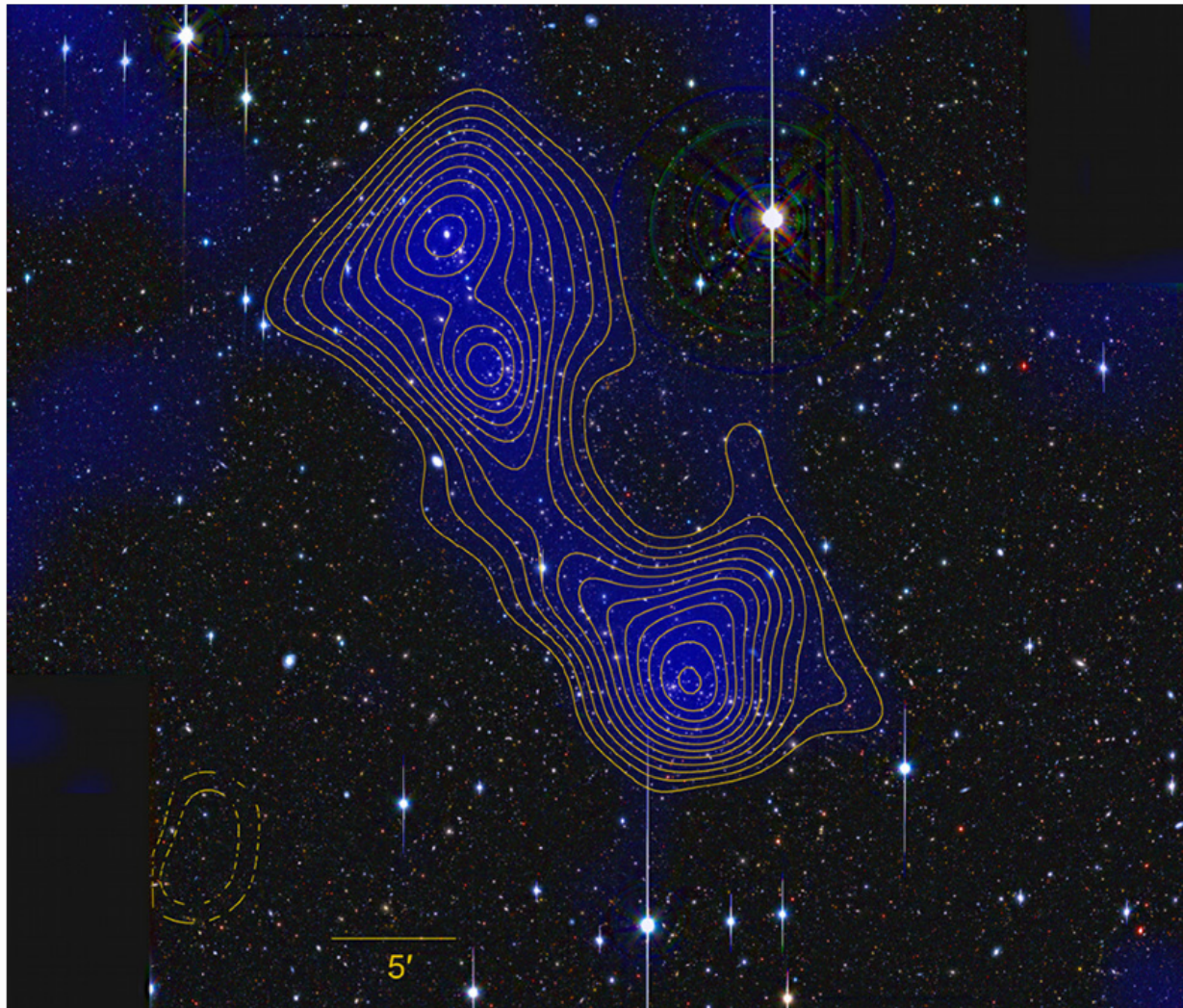
(von der Linden et al. 2014) — MACS\_J1621+3810, ground-based data,  
 $n_{\text{gal}} = 2.5 \dots 25 \text{ arcmin}^{-2}$

# Weak-lensing resolution



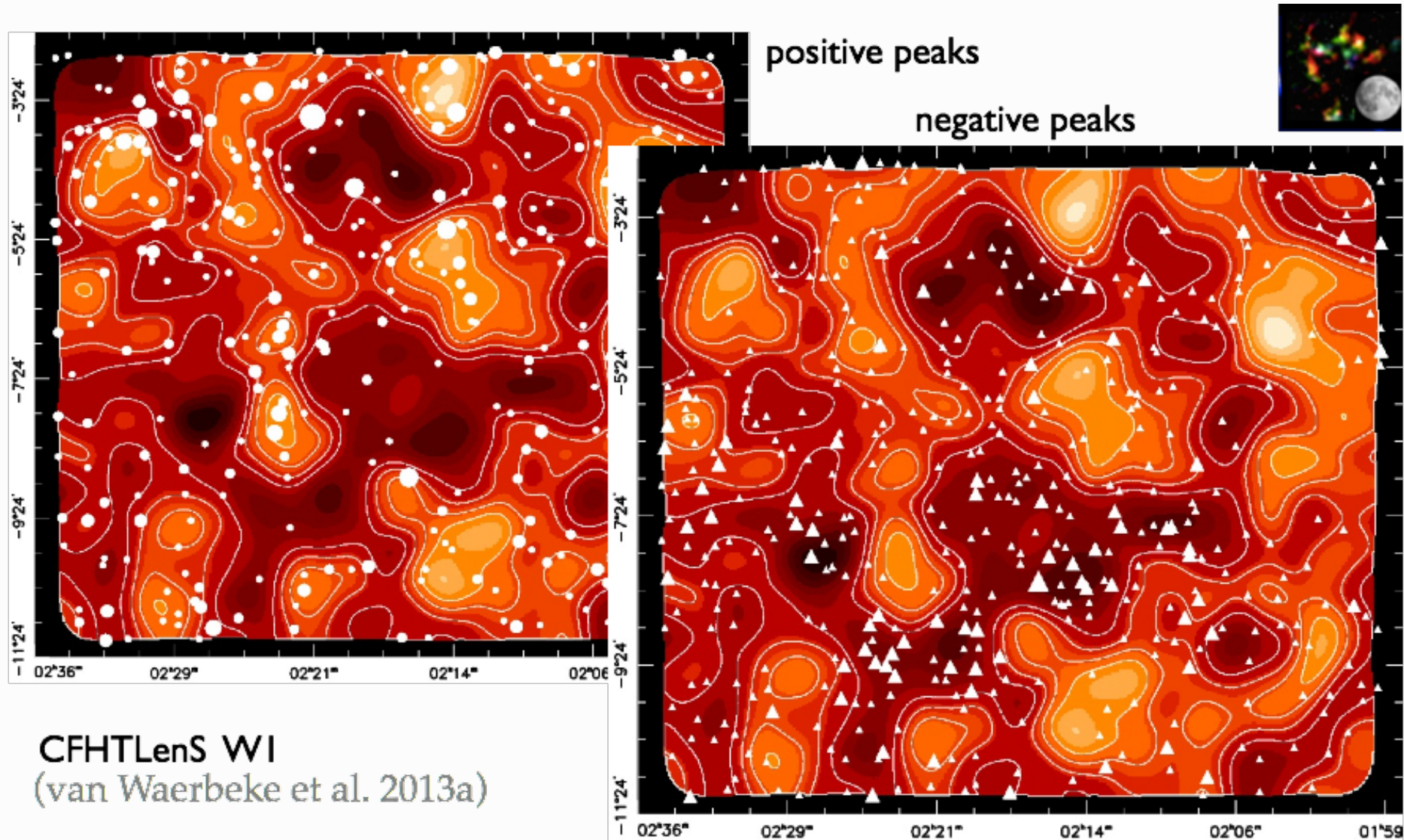
(Bonamente et al. 2012) — X- and SZ

# Weak-lensing resolution



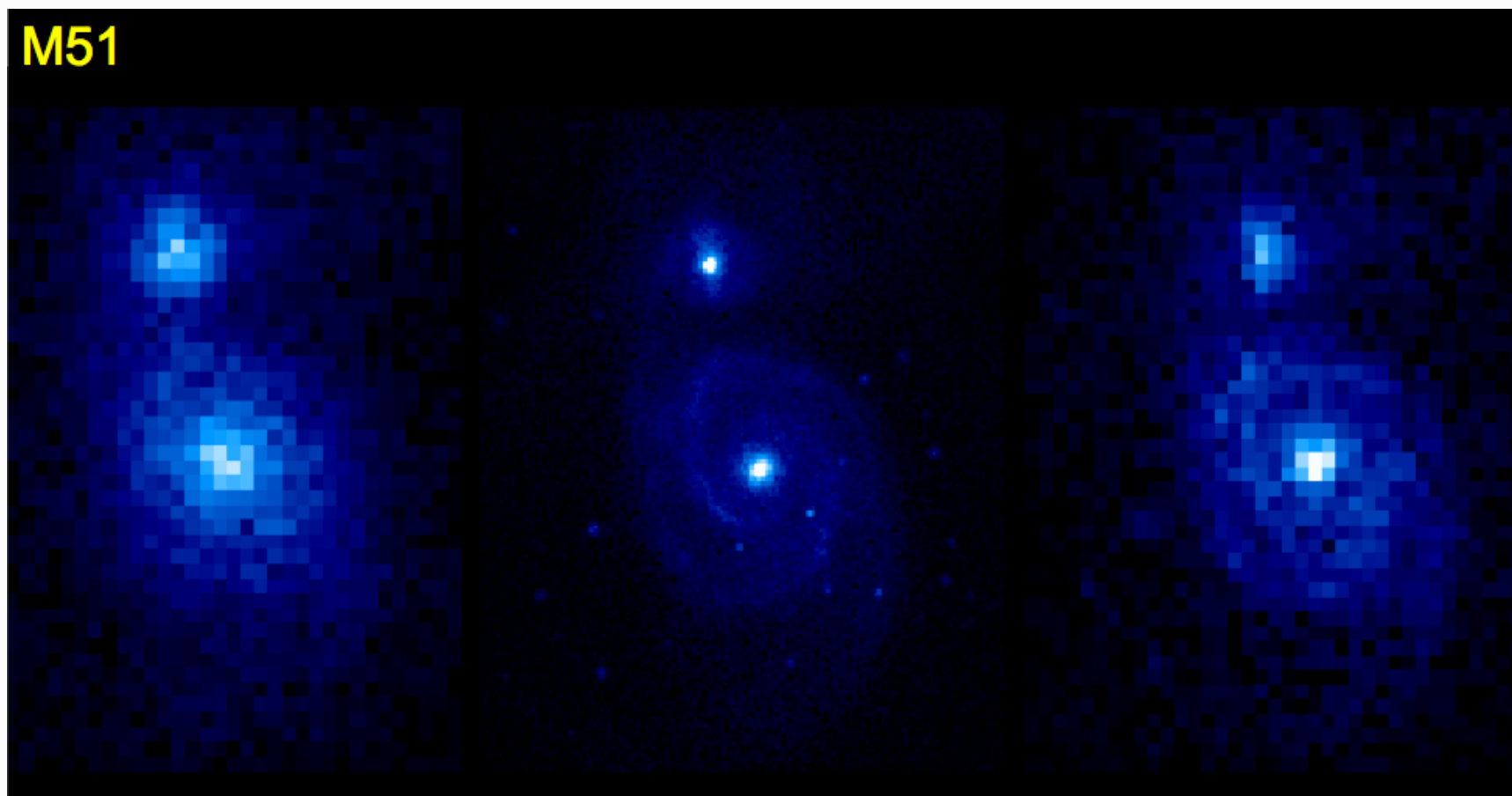
A 222/223, filament between clusters (Dietrich et al. 2012)

# Mass maps from CFHTLenS



# Euclid imaging

M51



SDSS @  $z=0.1$

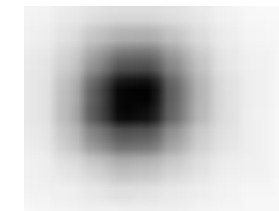
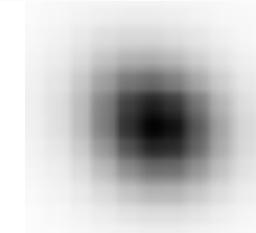
Euclid @  $z=0.1$

Euclid @  $z=0.7$

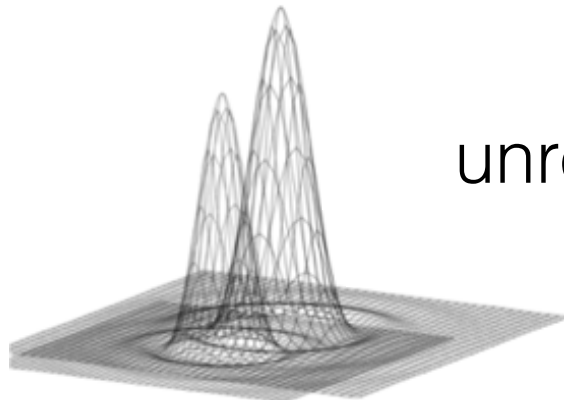
- Euclid images of  $z \sim 1$  galaxies: same resolution as SDSS images at  $z \sim 0.05$  and at least 3 magnitudes deeper.
- Space imaging of Euclid will outperform any other surveys of weak lensing.

## Some Euclid WL challenges

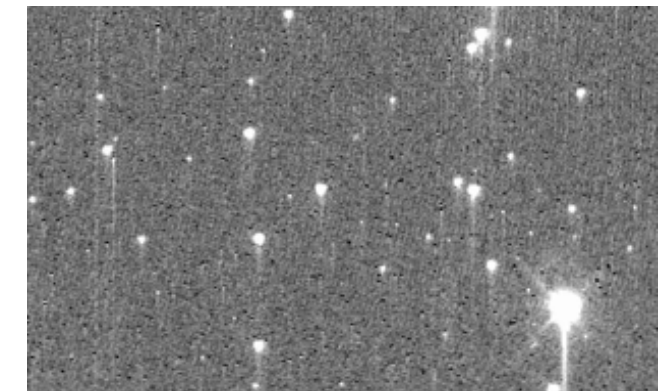
under-sampled PSF



unresolved binary stars



CTI  
(charge transfer inefficiency)

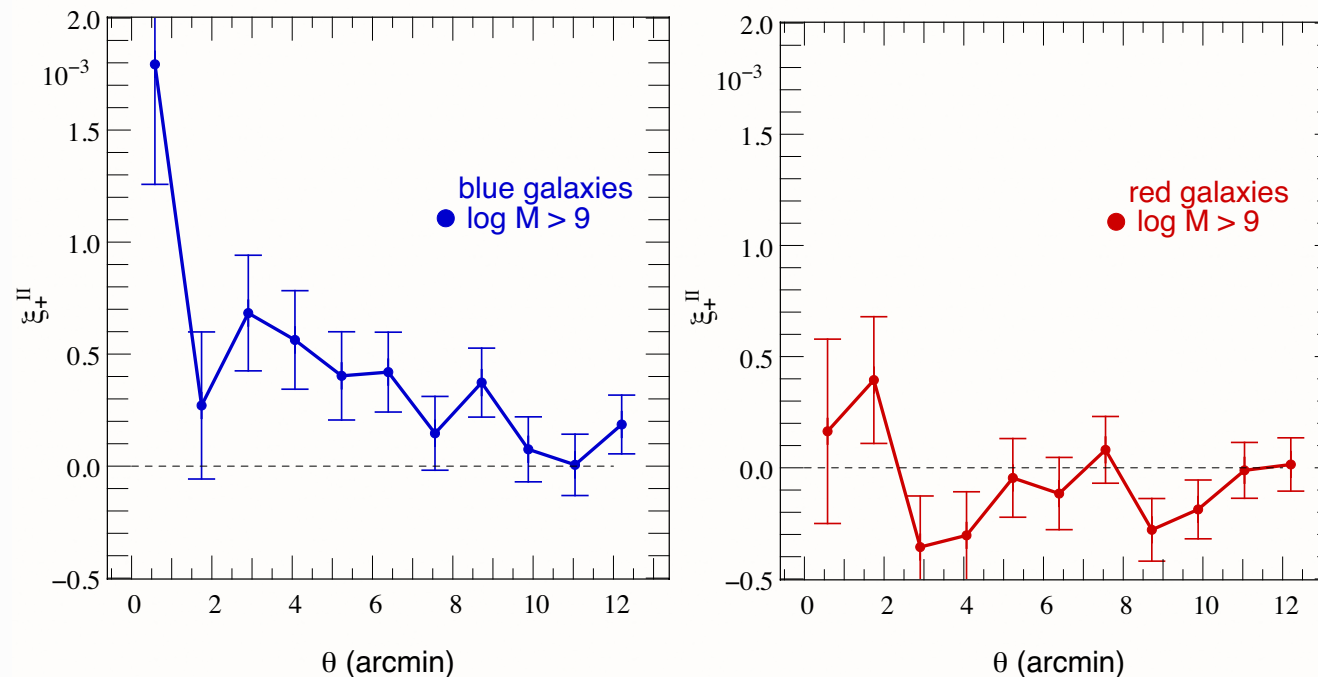


color gradients

# Open questions (selection) I

## Modelling

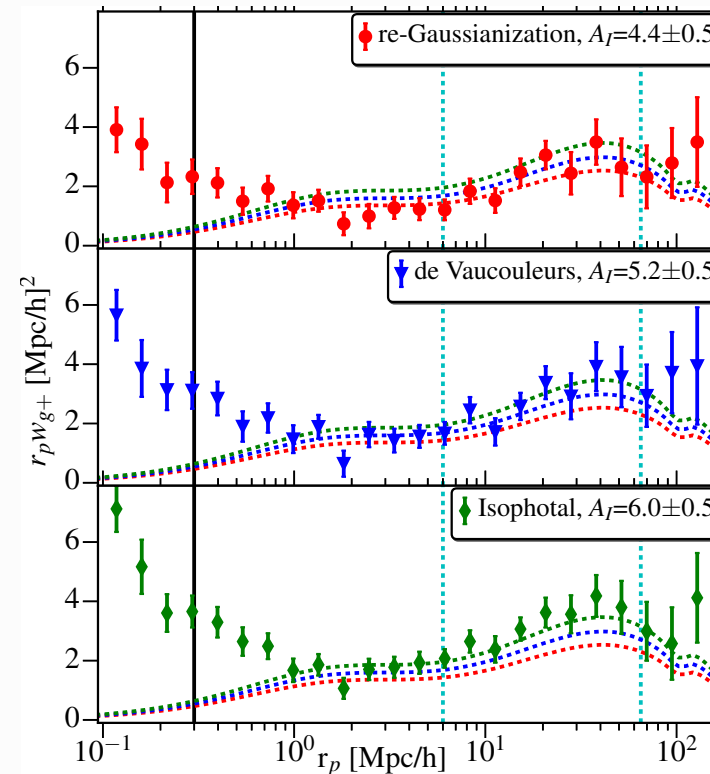
- Intrinsic alignment. Dependence on  $L$ , type,  $z$ ? Physically motivated model.  $N$ -body simulations.



(Codis et al. 2015)

## Open questions (selection) II

- IA contamination depends on shape measurement method!



(Singh & Mandelbaum 2016)

# Open questions (selection) III

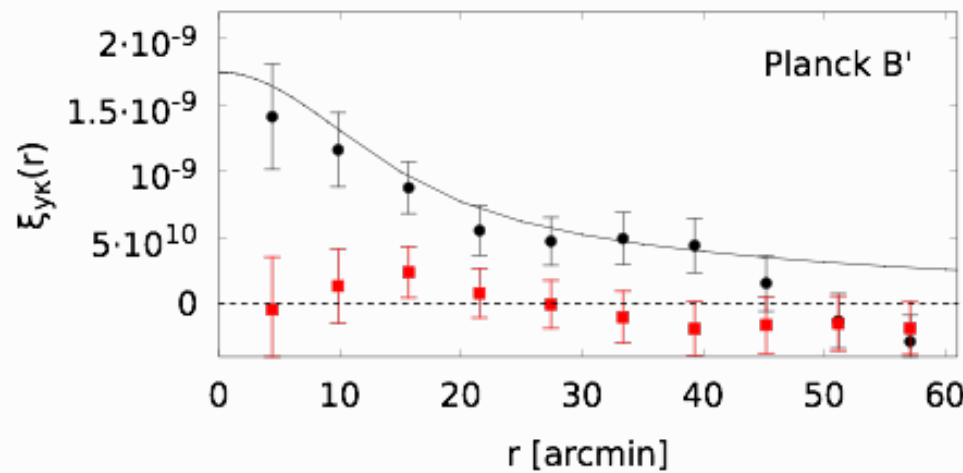
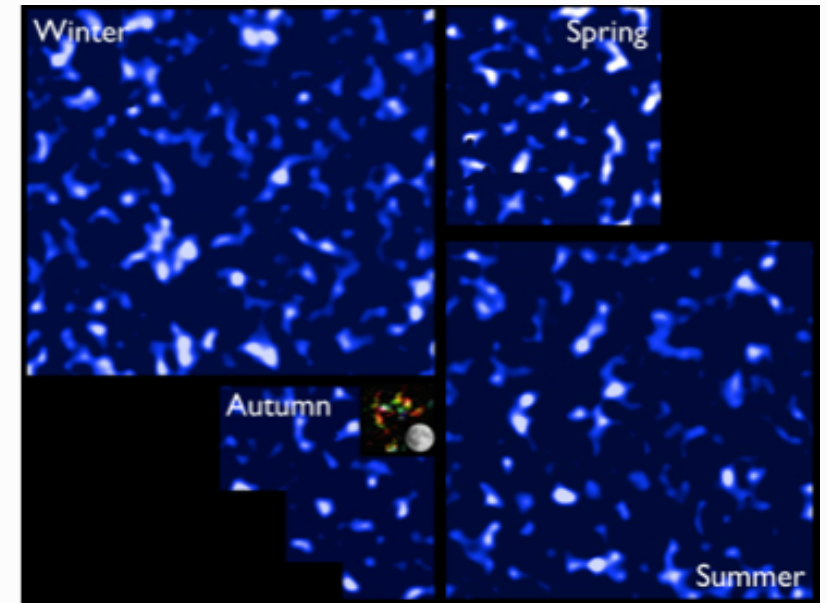
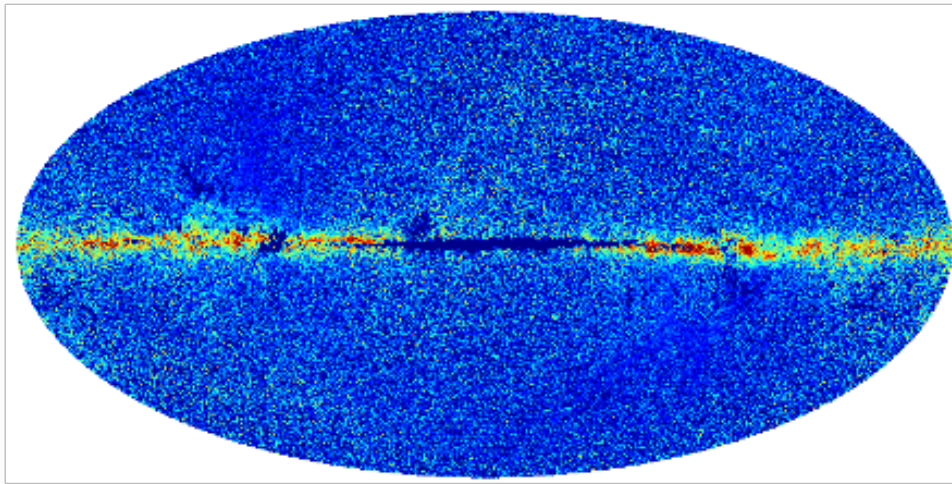
- Baryonic feedback in clusters, influence on WL, modelling.

## Photometric redshifts

- Euclid needs (very deep!) ground-based follow-up in multiple optical bands. Data (DES, KiDS, CFIS, ...) will be inhomogeneous. Problem of reliable photo- $z$ 's not yet solved.

# Further possible topics

1. E- and B-modes (what has been skipped yesterday)
2. CMB (x) lensing
3. Cluster weak lensing
4. Nature of dark matter (bullet cluster)
5. Testing GR with WL and galaxy clustering
6. Higher-order statistics: peak counts

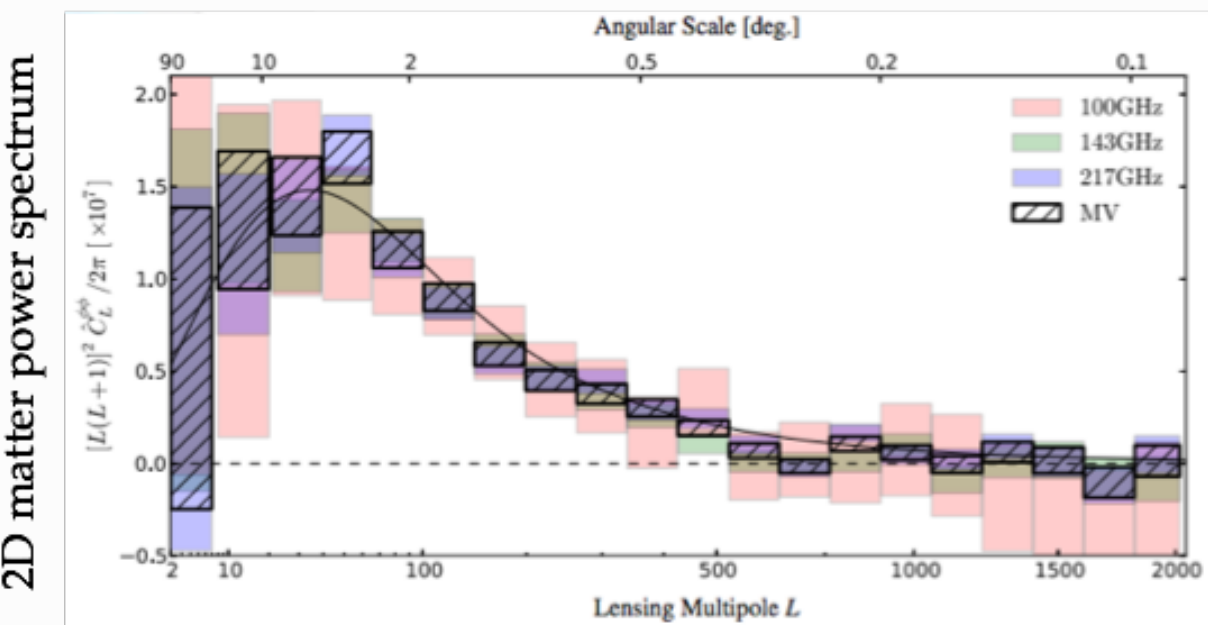
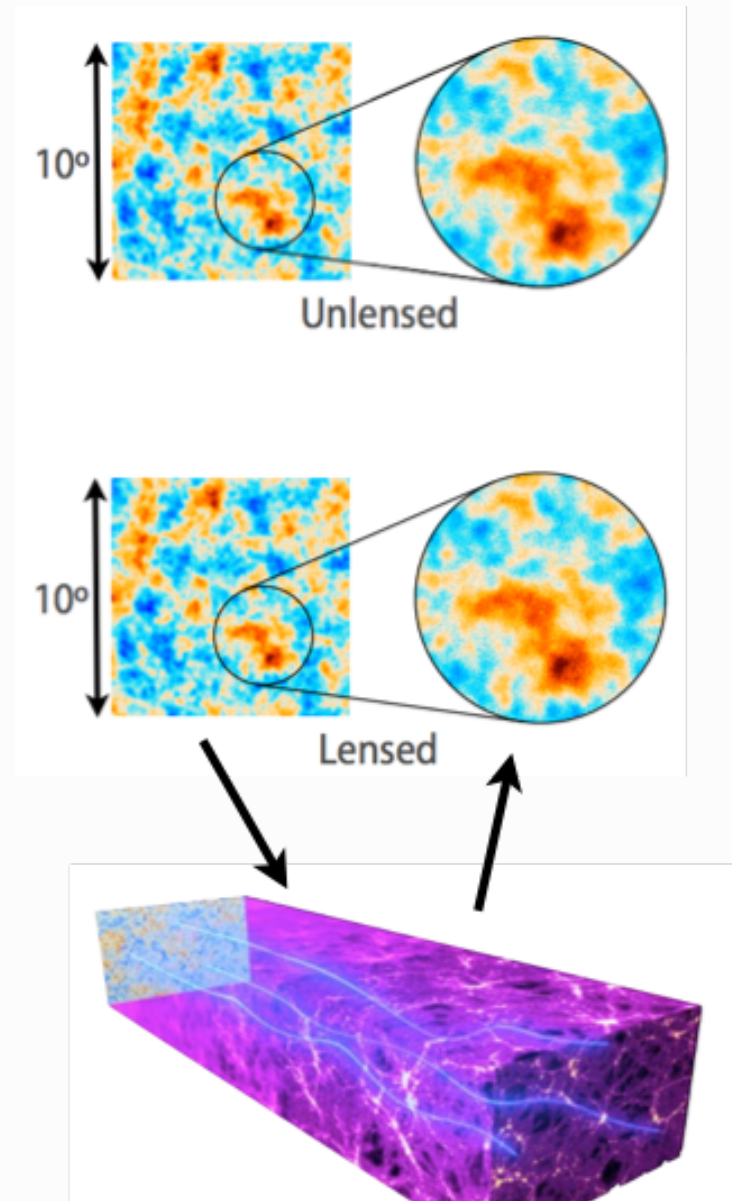
CMB (SZ)  $\times$  WL

$$\left(\frac{b_{\text{gas}}}{1}\right) \left(\frac{T_e(0)}{0.1 \text{ keV}}\right) \left(\frac{\bar{n}_e}{1 \text{ m}^{-3}}\right) = 2.01 \pm 0.31 \pm 0.21$$

(van Waerbeke et al. 2013b)

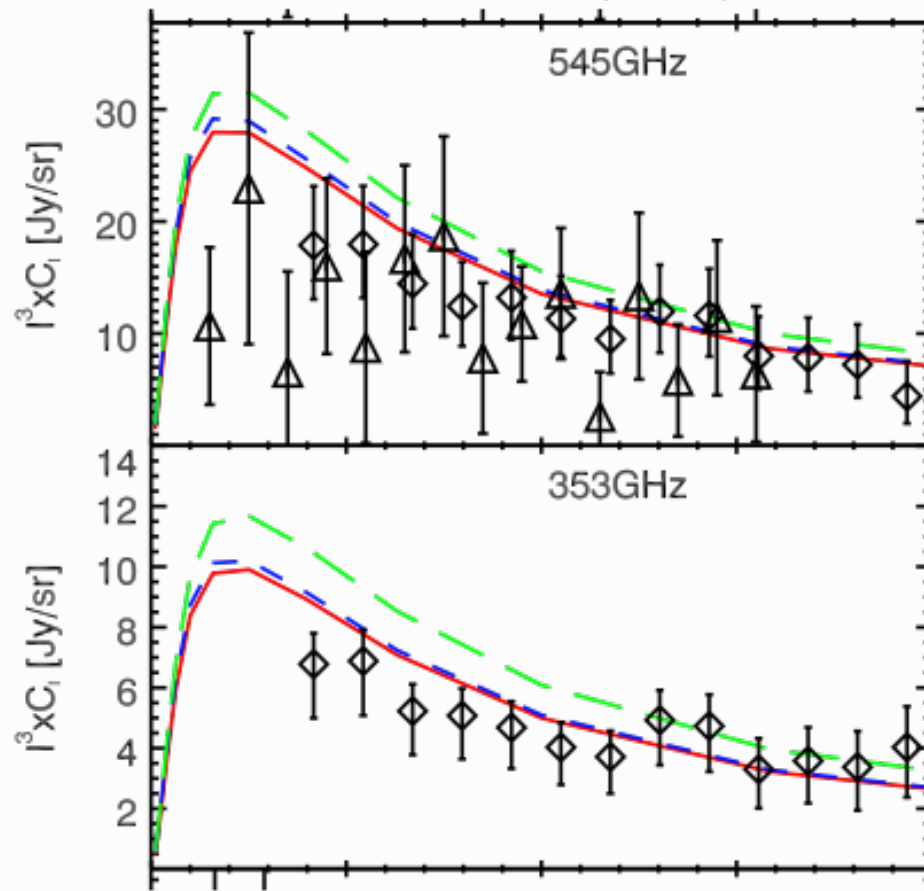
Planck CMB (SZ)  $\times$  CFHTLenS weak-lensing: hot gas associated with matter

# CMB lensing



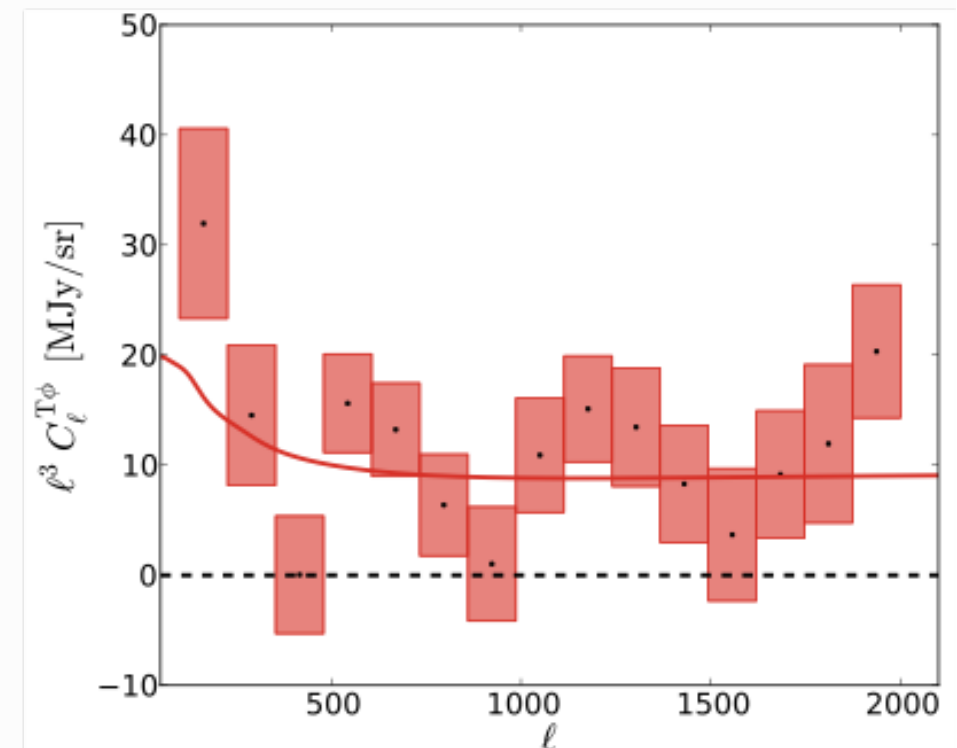
# CMB lensing

Béthermin et al. (2013)  
 Planck Consortium (2014)  
 Holder et al. (2014)



SPT CMB lens x Herschel CIB

Planck Consortium (2014)



# Stacked cluster weak lensing: Large scales

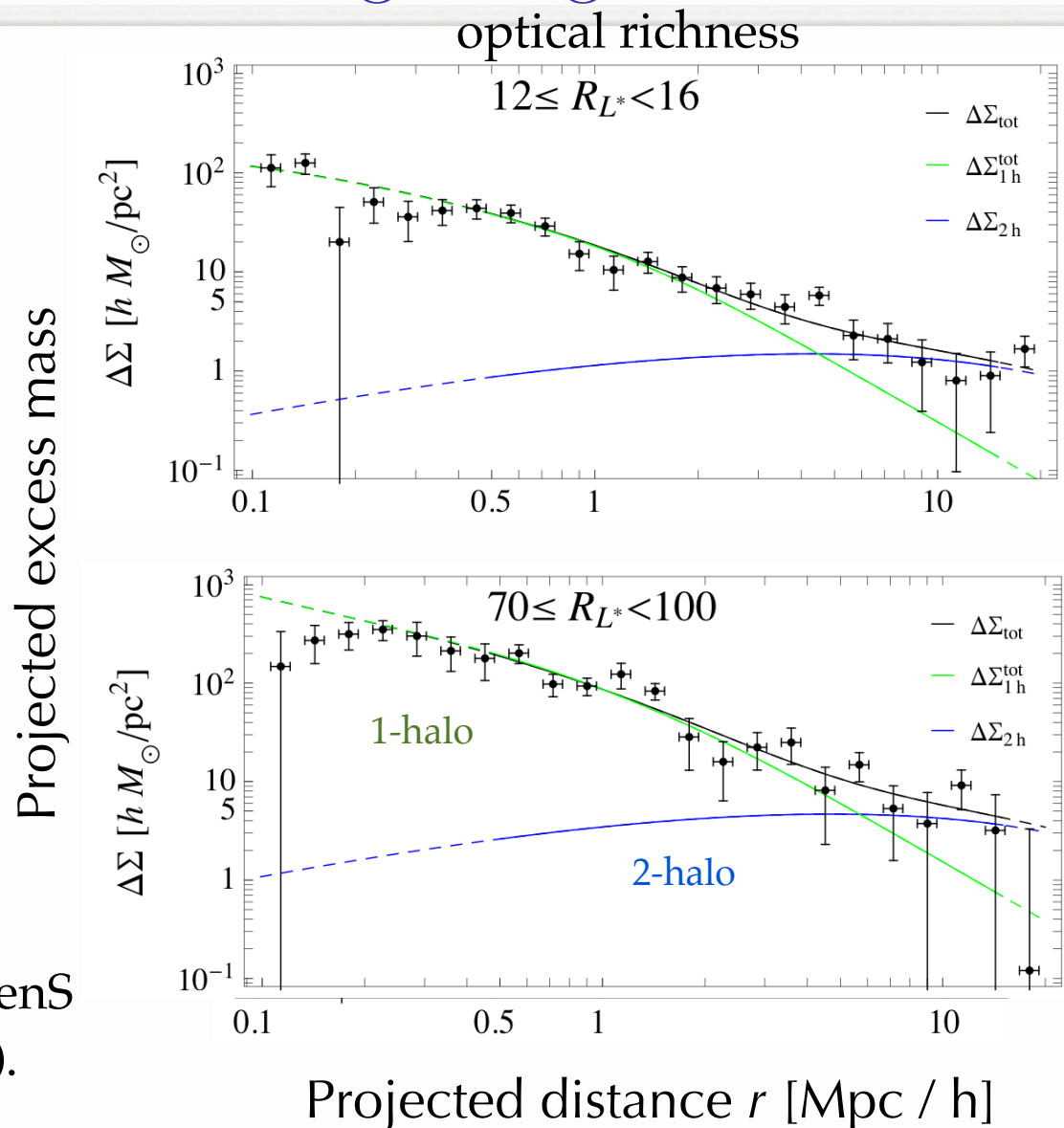
Weak lensing measures mass associated with clusters.

At large distances: excess mass in nearby, correlated clusters  
 → clustering of galaxy clusters.

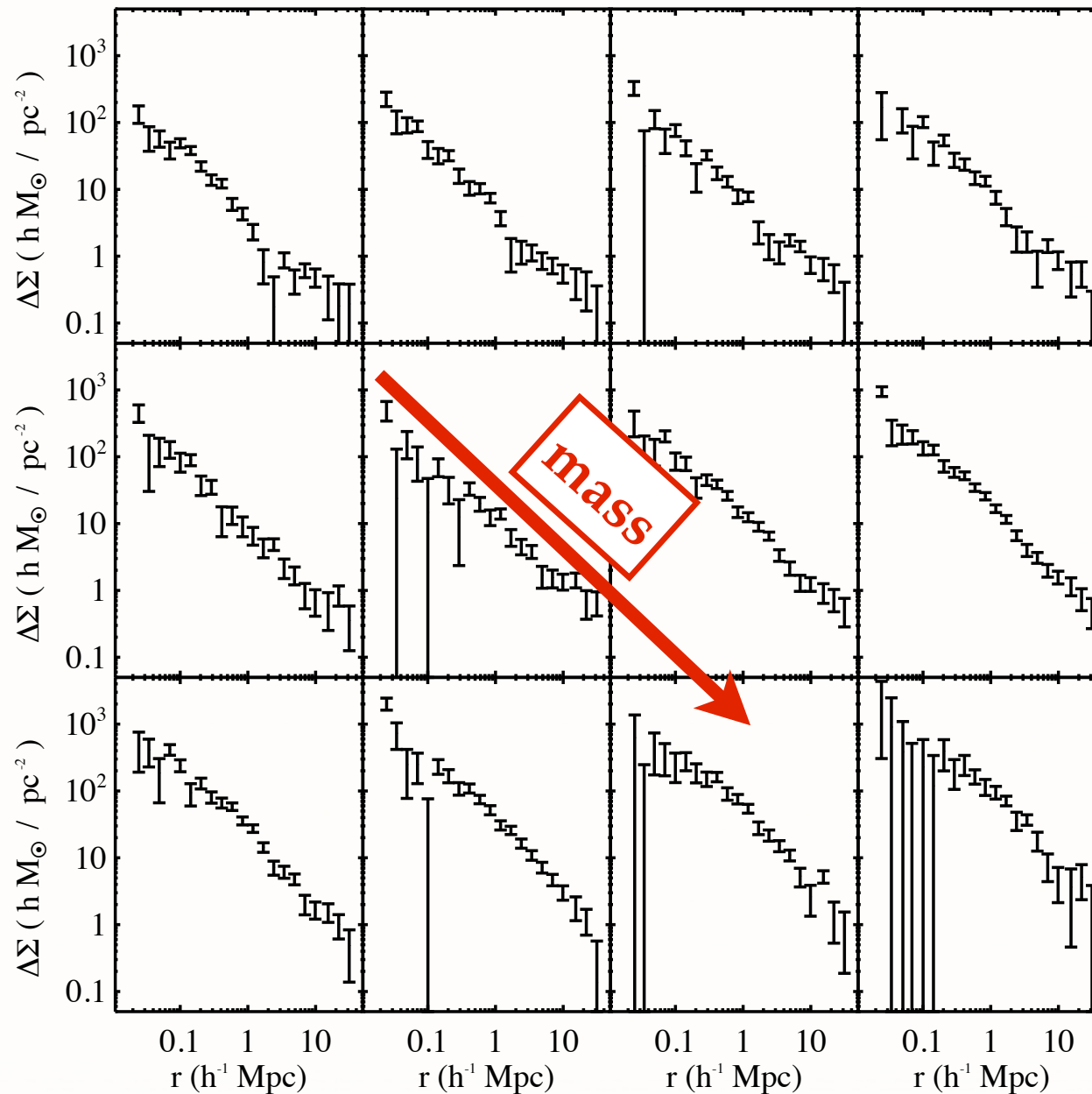
bg shear - fg position  $\sim b_h \sigma_8^2$   
 halo bias, function of mass

1200 clusters in  $150 \text{ deg}^2$  CFHTLenS area,  $0.1 < z < 0.6$  (mean  $z = 0.37$ ).

Covone, Sereno, MK & Cardone (2014)



# Stacked cluster weak lensing: 2D mass profiles



Bin number	$N_{200}$
1	3
2	4
3	5
4	6
5	7
6	8
7	9-11
8	12-17
9	18-25
10	26-40
11	41-70
12	71-220

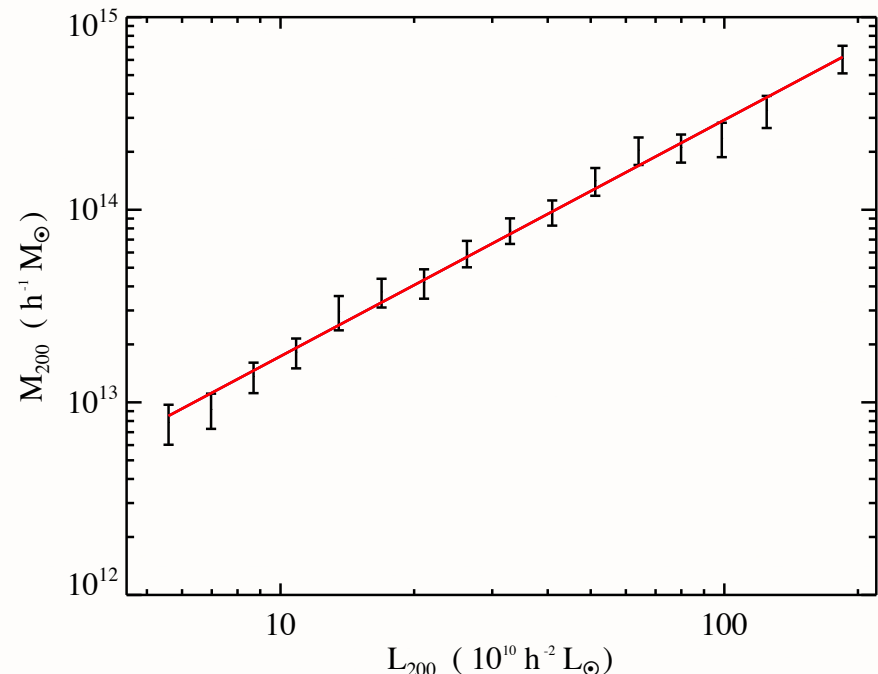
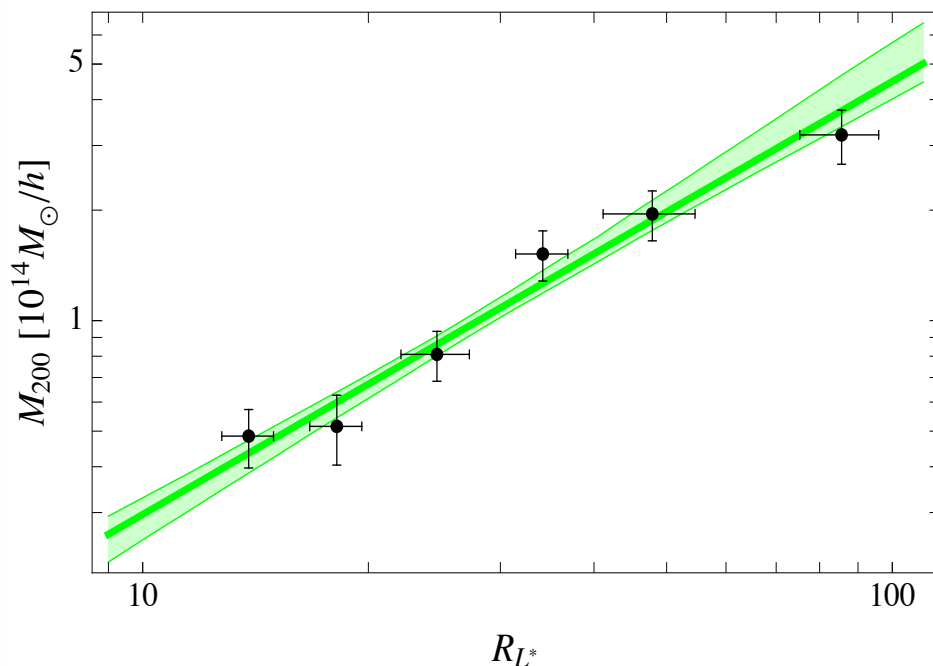
130,000 clusters in  
of SDSS  $\sim 6,000 \text{ deg}^2$   
at  $z=0.25$

Johnston et al. (2009)

# Stacked cluster weak lensing: Scaling relations

Covone et al. (2014)

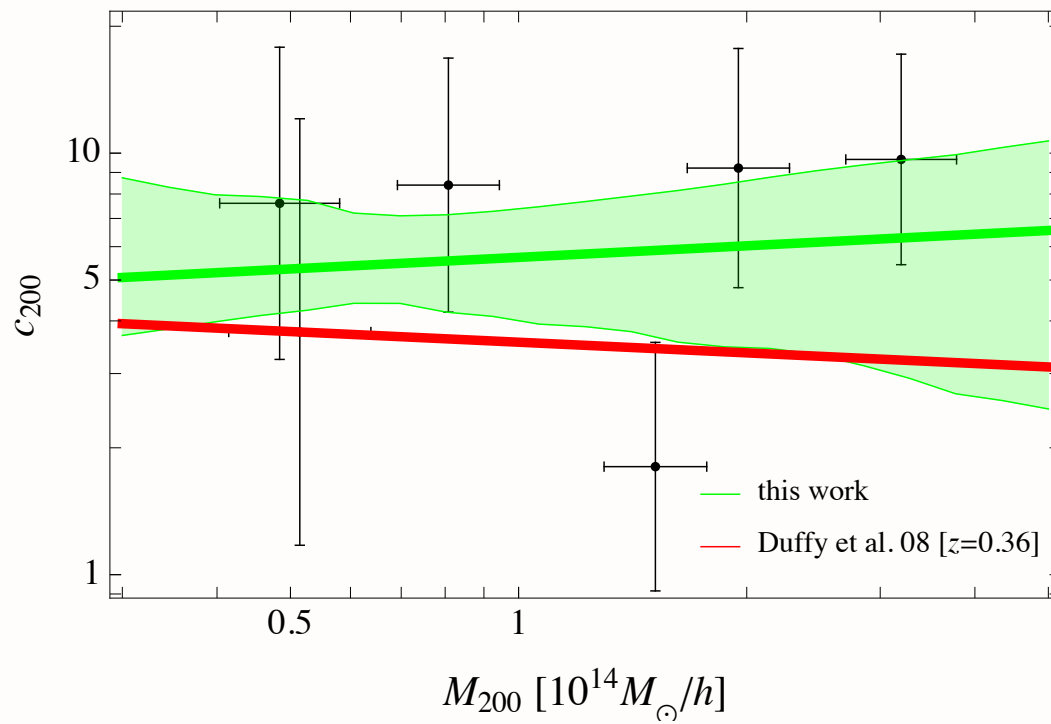
Johnston et al. (2009)



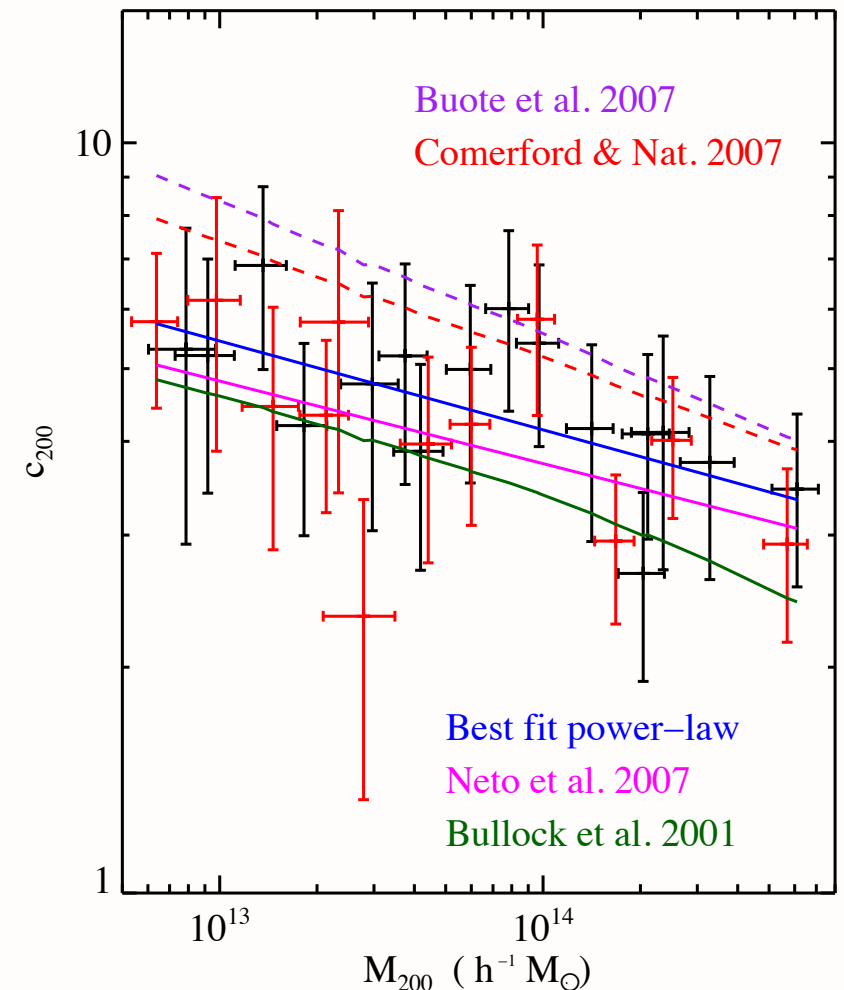
- Scaling relations, necessary calibrating (mass - observable) for cosmology
- XXL (M. Pierre):  $\sim 100$  X-ray selected clusters,  $25 \text{ deg}^2$  overlap with CFHTLS, compare lensing and X-ray derived masses.

# Stacked cluster weak lensing on large scales

Covone et al. (2014)



Johnston et al. (2009)

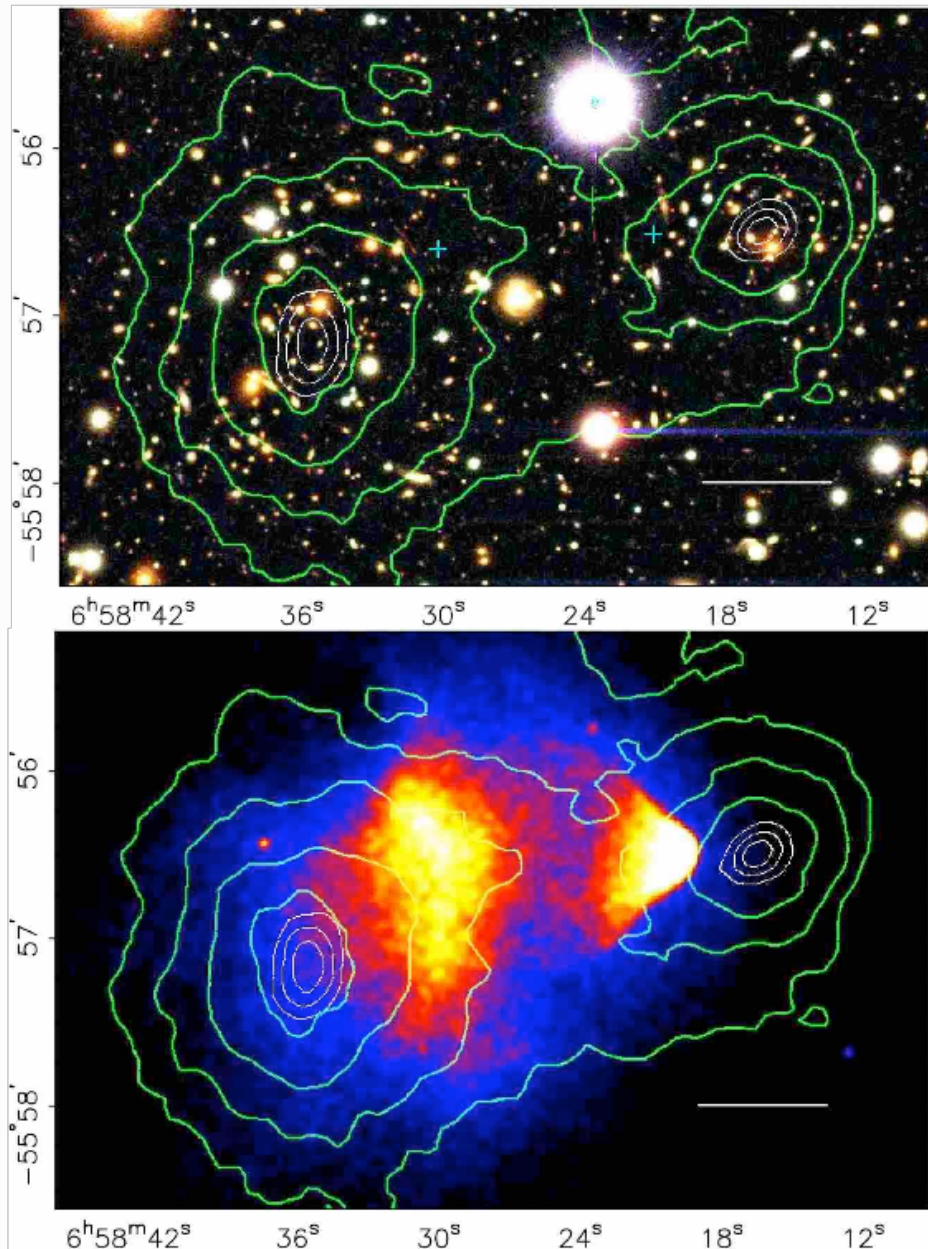


- Concentration parameter  $c$  reflects central halo density; depends on assembly history, formation time
- Predictions usually from  $N$ -body simulations
- Indirect test of CDM paradigm

# The bullet cluster and the nature of dark matter



# The bullet cluster



- Merging galaxy cluster at  $z = 0.296$
- Recent major merger 100 Myr ago
- Components moving nearly perpendicular to line of sight with  $v = 4700 \text{ km s}^{-1}$
- Galaxy concentration offset from X-ray emission. Bow shocks visible

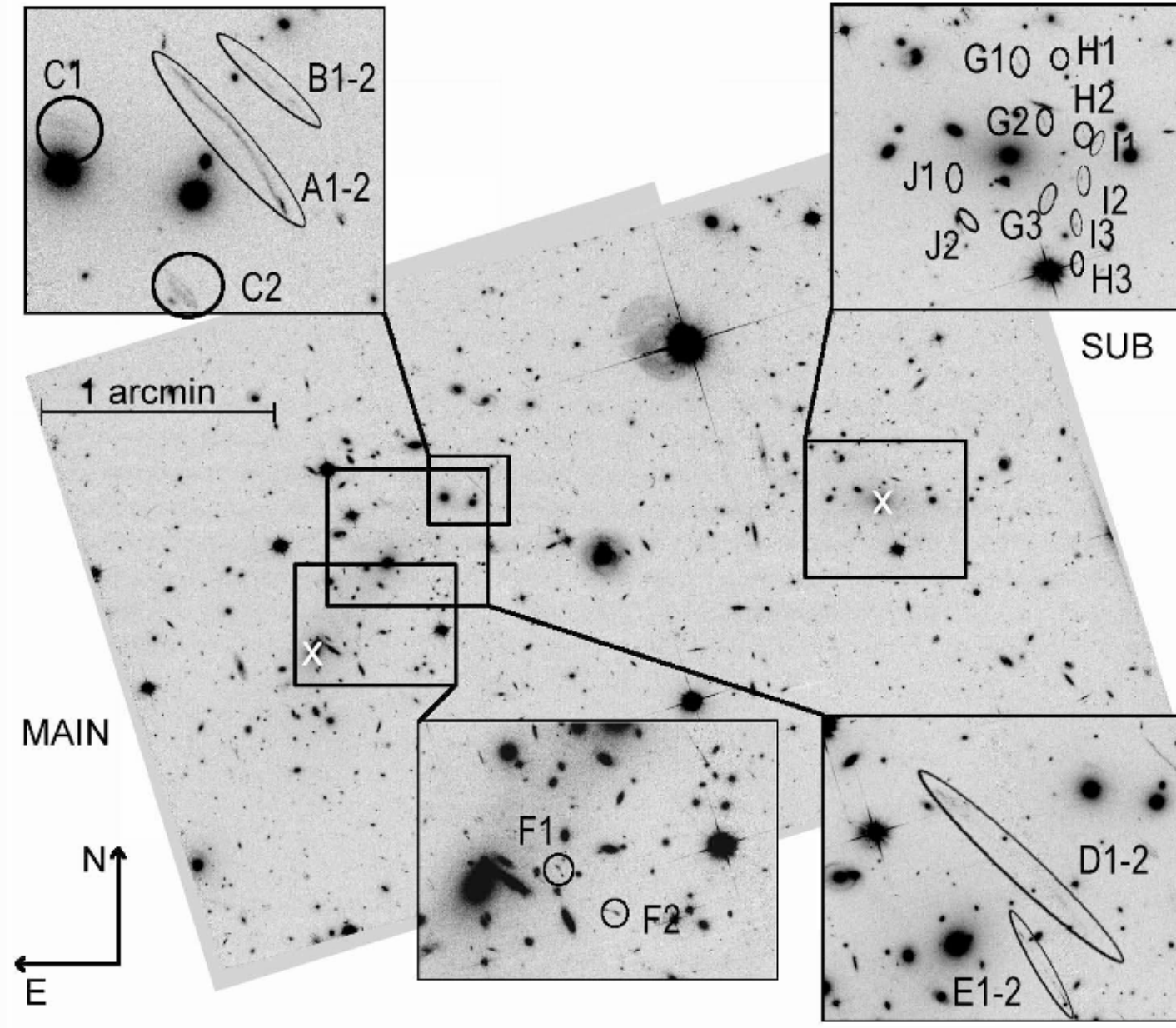
Clowe et al. (2006)

# The bullet cluster: SL+WL measurements

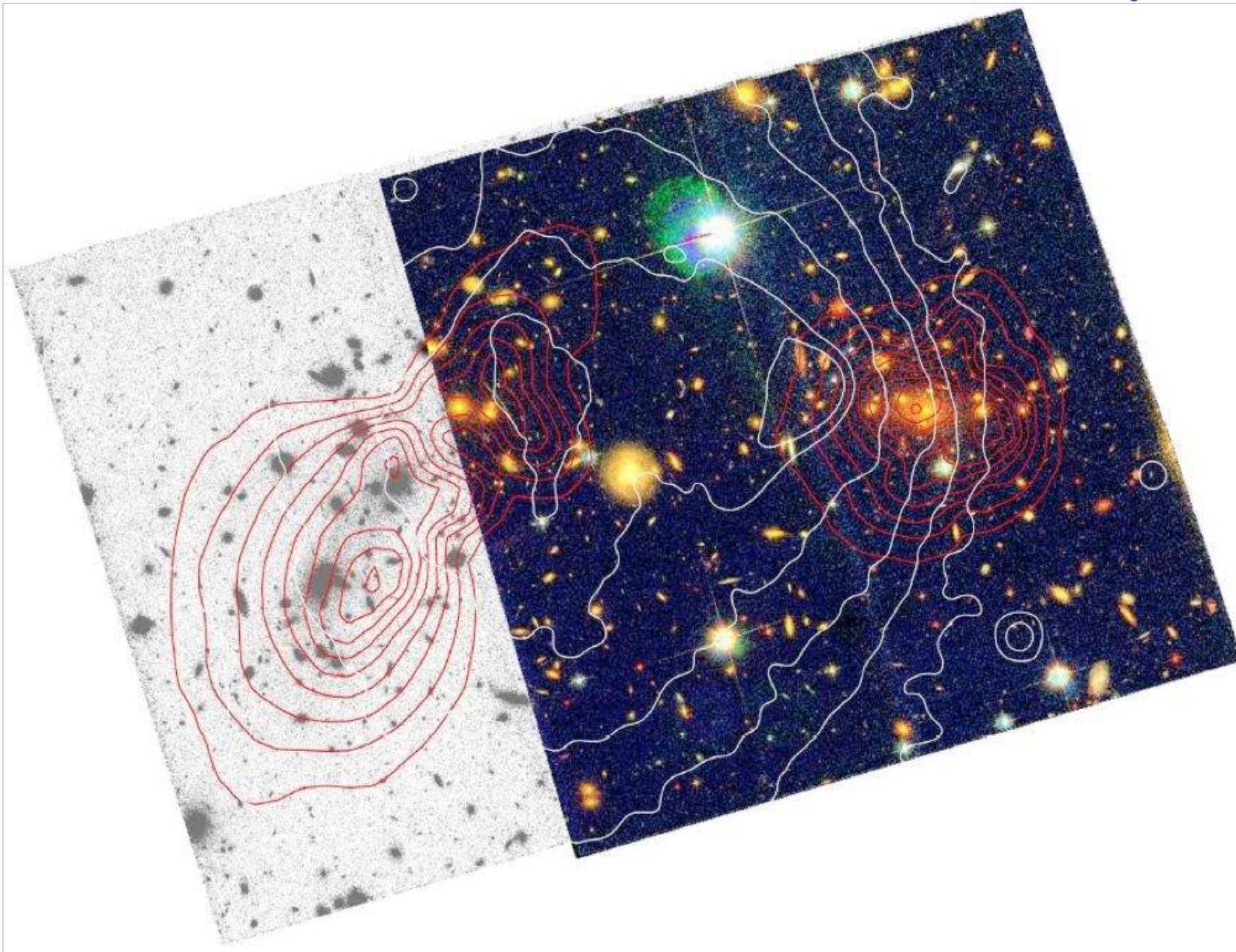
Instrument	Date of Obs.	FoV	Passband	$t_{\text{exp}}$ (s)	$m_{\text{lim}}$	$n_d$ (' $^{-2}$ )	seeing
2.2m ESO/MPG Wide Field Imager	01/2004	$34' \times 34'$	R	14100	23.9	15	0. $''$ 8
	01/2004		B	6580			1. $''$ 0
	01/2004		V	5640			0. $''$ 9
6.5m Magellan IMACS	01/15/2004	8' radius	R	10800	25.1	35	0. $''$ 6
	01/15/2004		B	2700			0. $''$ 9
	01/15/2004		V	2400			0. $''$ 8
HST ACS subcluster	10/21/2004	3. $'$ 5×3. $'$ 5	F814W	4944	27.6	87	0. $''$ 12
	10/21/2004		F435W	2420			0. $''$ 12
	10/21/2004		F606W	2336			0. $''$ 12
main cluster	10/21/2004	3. $'$ 5×3. $'$ 5	F606W	2336	26.1	54	0. $''$ 12

(Bradač et al. 2006, Clowe et al. 2006)

# The bullet cluster: strong lensing



# The bullet cluster: WL and X-ray



# The bullet cluster: Evidence for dark matter

- $10\sigma(6\sigma)$  offset between main (sub-)mass peak and X-ray gas → most cluster mass is not in hot X-ray gas (unlike most baryonic mass:  $m_X \gg m_*$ !)
- Main mass associated with galaxies → this matter is collisionless

Modified gravity theories without dark matter: MoND (Modified Newtonian Dynamics), (Milgrom 1983), changes Newton's law for low accelerations ( $a \sim 10^{-10} \text{ m s}^{-2}$ ), can produce flat galaxy rotation curves and Tully-Fisher relation.

MoND's relativistic version (Bekenstein 2004), varying gravitational constant  $G(r)$ . Introduces new vector field ("phion") with coupling strength  $\alpha(r)$  and range  $\lambda(r)$  as free functions.

This can produce non-local weak-lensing convergence mass, where  $\kappa \not\propto \delta$ !

Necessary to explain offset between main  $\kappa$  peak and main baryonic mass.

Model with four mass peaks can roughly reproduce WL map **with additional collisionless mass!** E.g. 2 eV neutrinos.

# The bullet cluster: MoND model

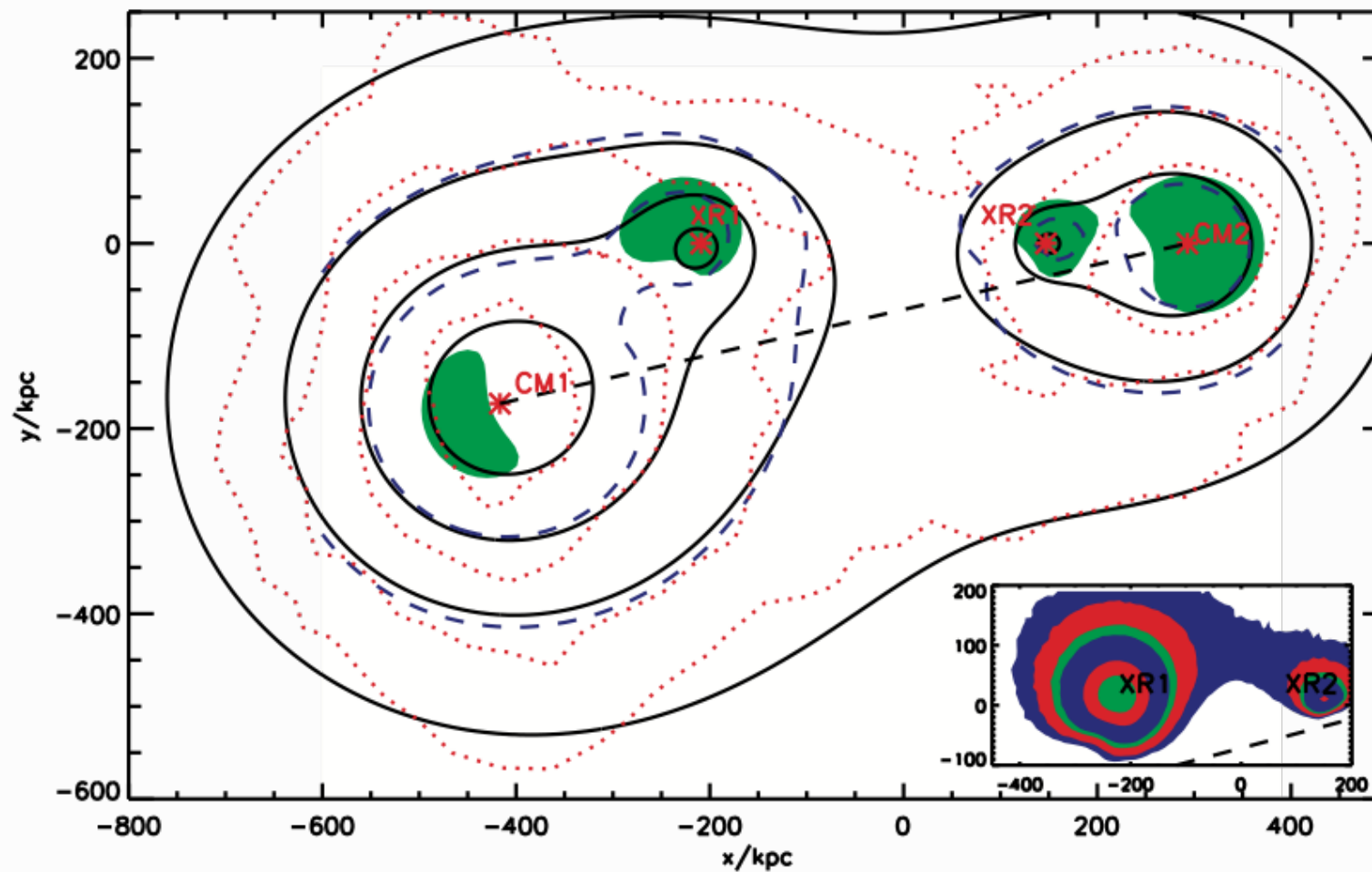
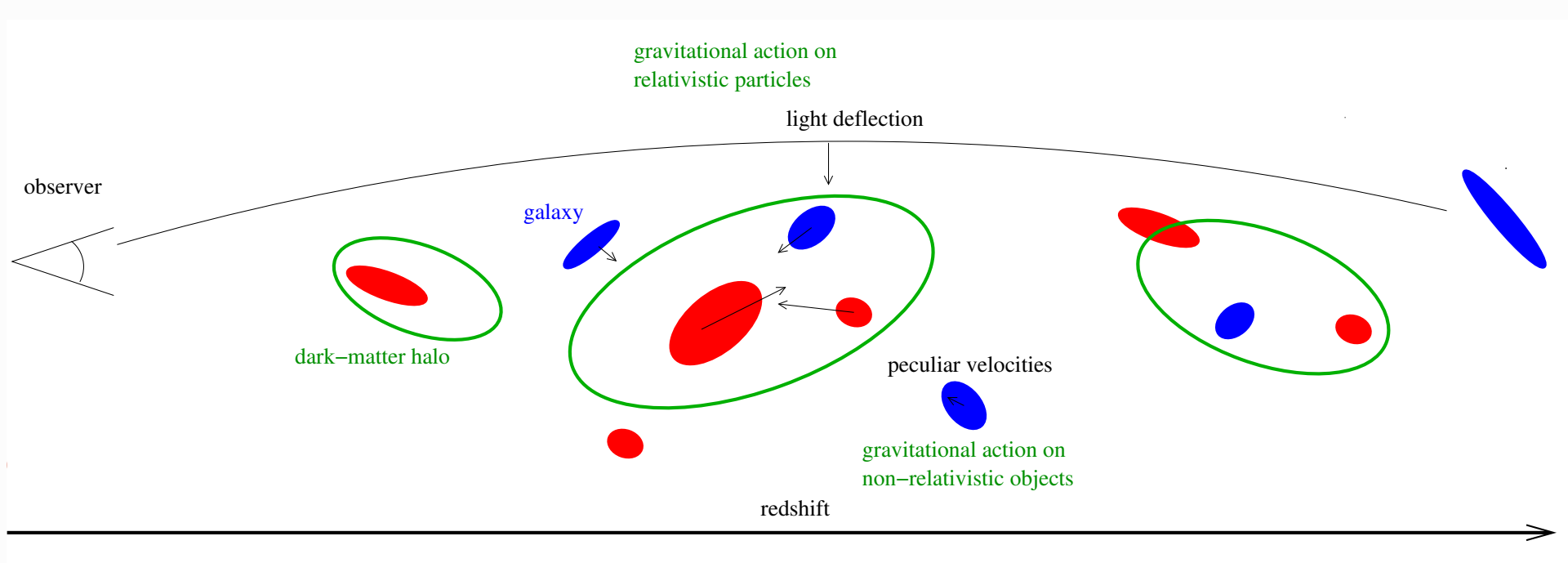


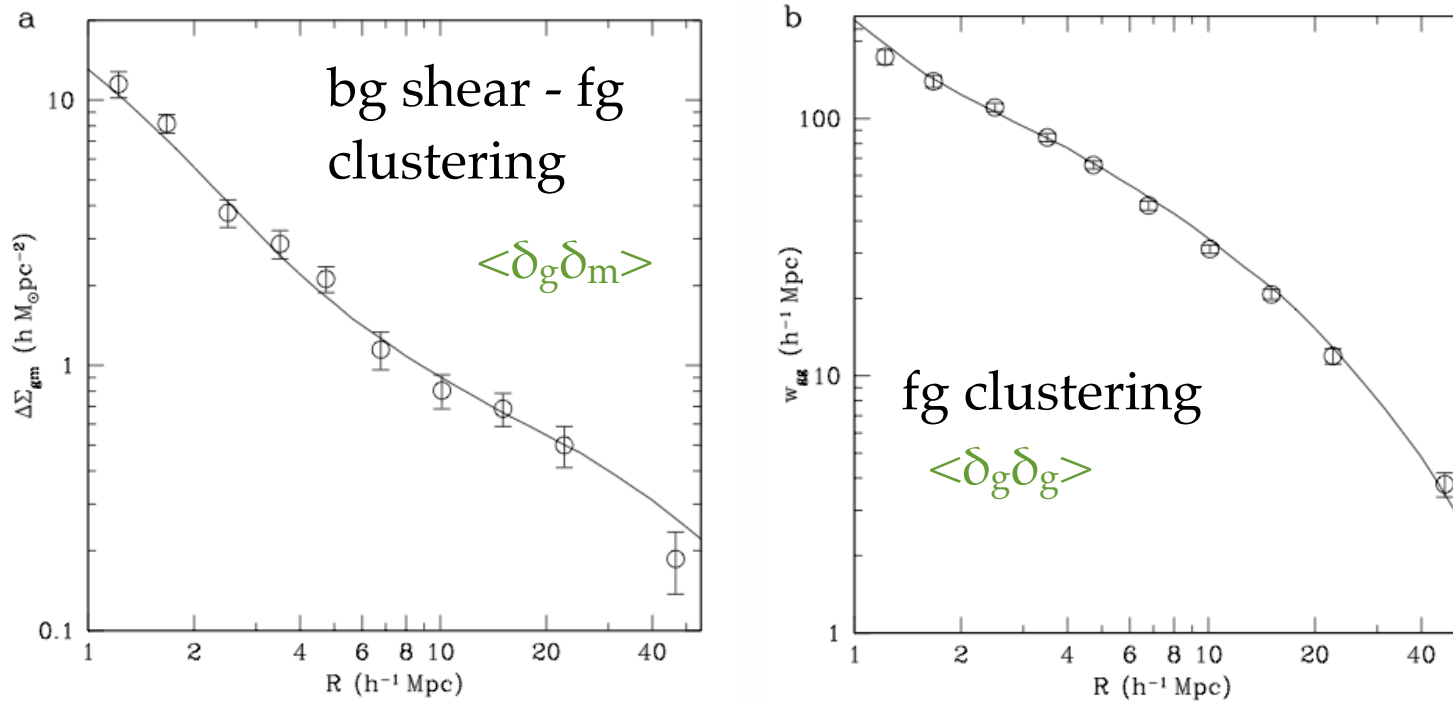
FIG. 1.— Our fitted convergence map (solid black lines) overplotted on the convergence map of C06 (dotted red lines) with x and y axes in kpc. The contours are from the outside 0.16, 0.23, 0.3 and 0.37. The centres of the four potentials we used are the red stars which are labelled. Also overplotted (blue dashed line) are two contours of surface density  $[4.8 \text{ & } 7.2] \times 10^2 M_\odot \text{ pc}^{-2}$  for the MOND standard  $\mu$  function; note slight distortions compared to the contours of  $\kappa$ . The green shaded region is where matter density is above  $1.8 \times 10^{-3} M_\odot \text{ pc}^{-3}$  and correspond to the clustering of 2eV neutrinos. *Inset:* The surface density of the gas in the bullet cluster predicted by our collisionless matter subtraction method for the standard  $\mu$ -function. The contour levels are  $[30, 50, 80, 100, 200, 300] M_\odot \text{ pc}^{-2}$ . The origin in RA and dec is  $[06^h 58^m 24.38^s, -55^\circ 56' 32]$

# Testing GR with WL and galaxy clustering



# Results from SDSS

SDSS (Reyes et al. 2010)



$$E_G \approx \frac{1}{\beta} \frac{\langle \delta_m \delta_g \rangle}{\langle \delta_g \delta_g \rangle}$$

galaxy bias

$$\beta = \frac{1}{b} \frac{d \ln D_+}{d \ln a}$$

$$\beta = 0.309 \pm 0.035$$

growth factor

from SDSS galaxy clustering  
(redshift-space distortions)  
Tegmark et al. (2006)

## Results from SDSS

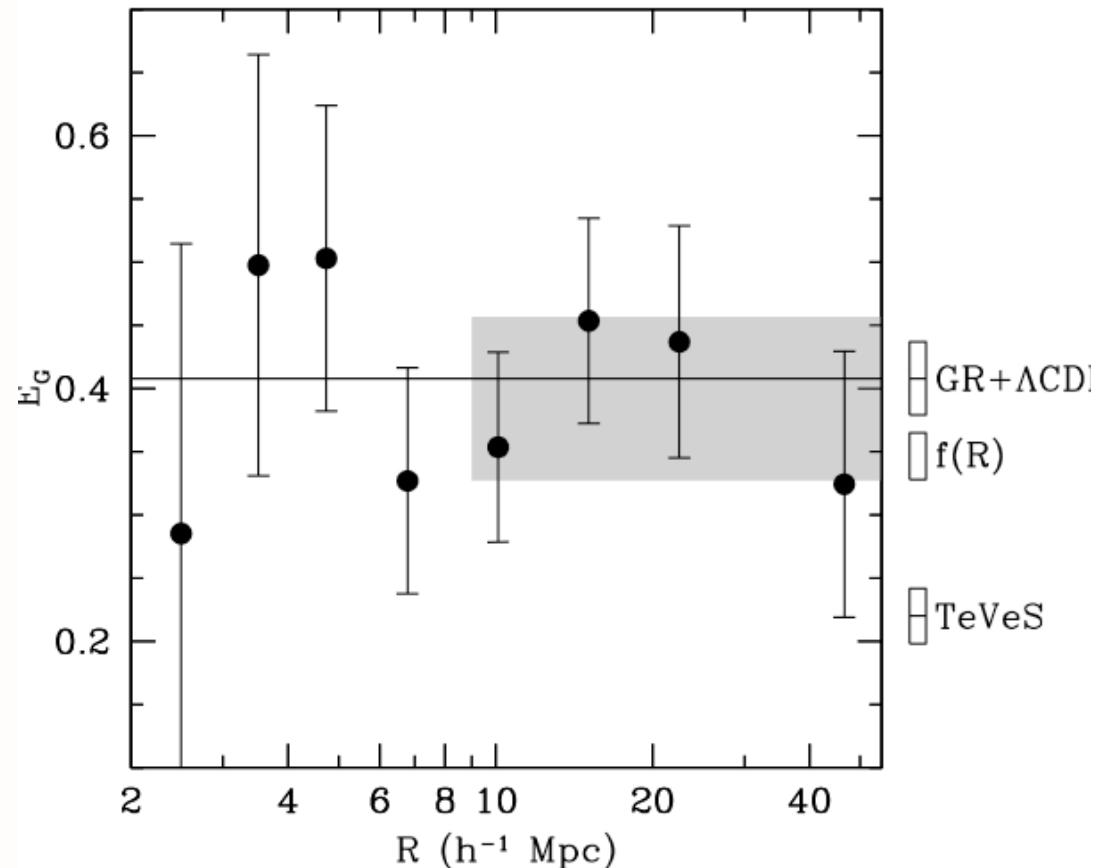
# Friedmann-Lemaître-Robertson-Walker metric with perturbations:

$$ds^2 = -(1 + 2\varphi)dt^2 + (1 - 2\phi)a^2dx^2$$

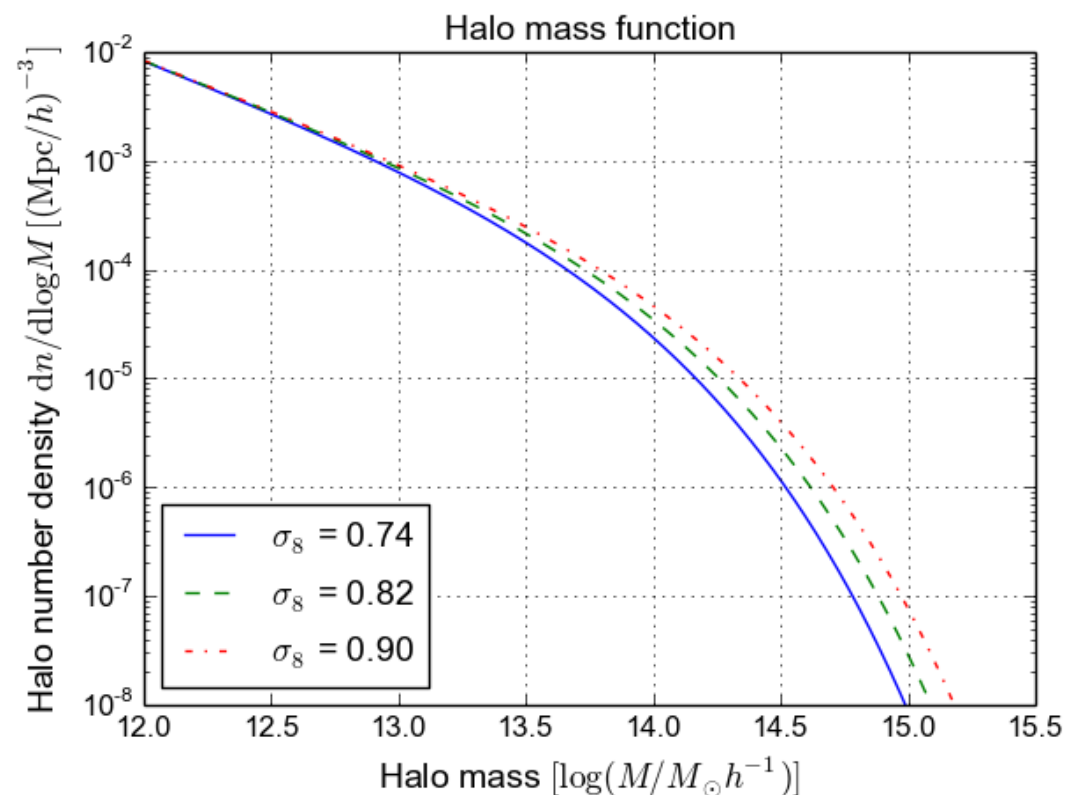
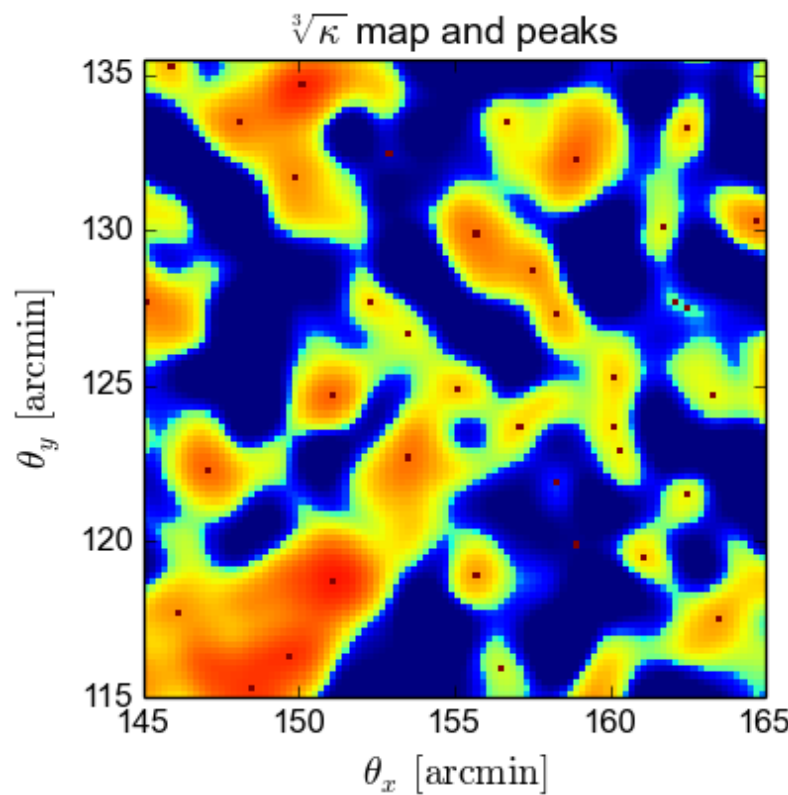
time dilation      spatial curvature

(Reyes et al. 201

- Galaxy-galaxy lensing:  
measures  $\phi$  +  $\varphi$  and  $b$
  - Galaxy clustering:  
measures  $\varphi$



# WL peak counts: Why do we want to study peaks?



- Local maxima of the projected mass
- Direct tracers of massive regions
- Probe mass function

# WL peak counts. What are peaks good for?

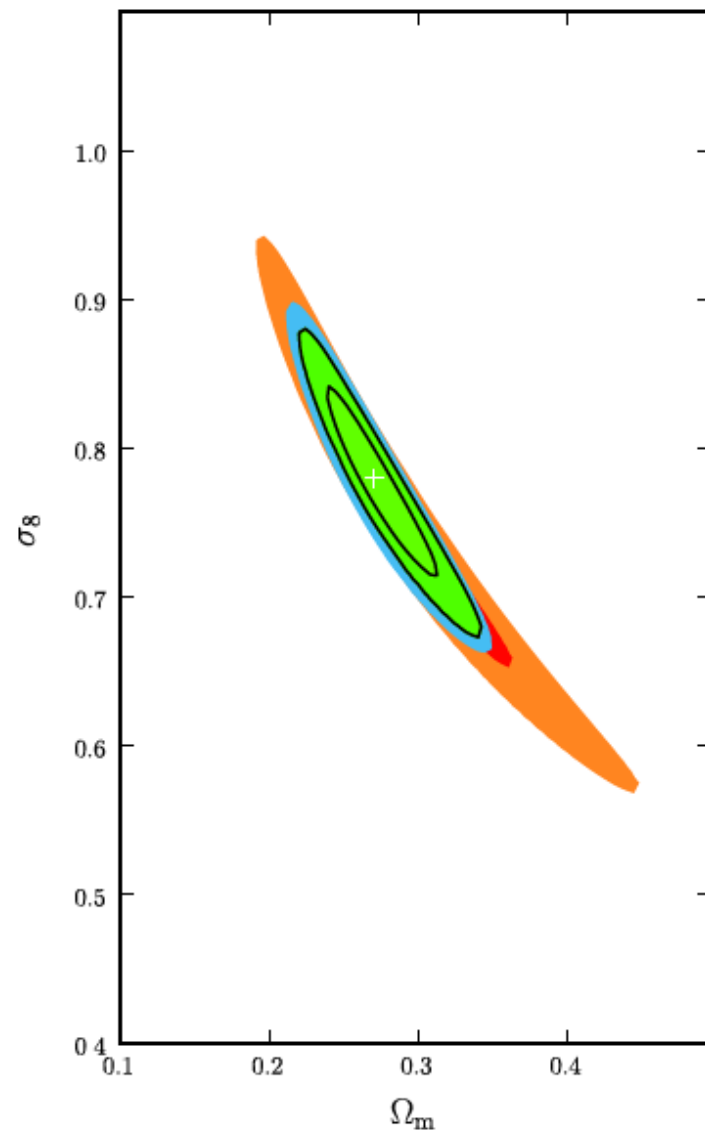
What do we gain from peak counting?

- Additional and complementary information and constraints compared to 2<sup>nd</sup> order shear
- Non-Gaussian information

Figure from Dietrich & Hartlap 2010

red/orange: cosmic shear

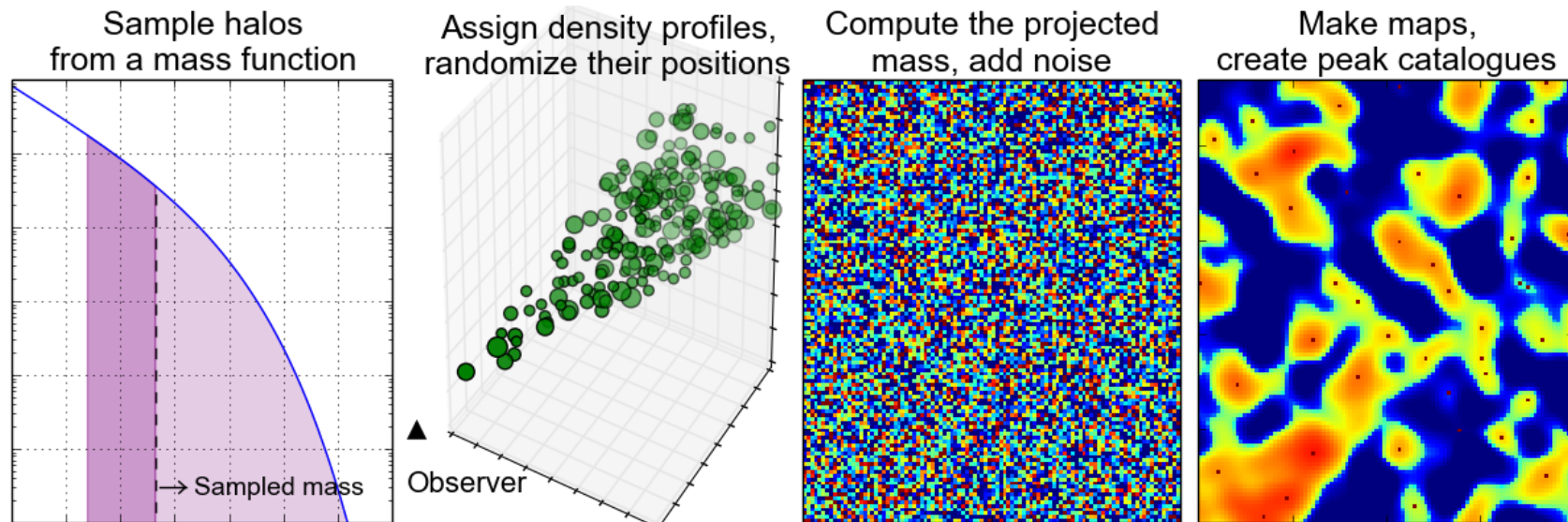
green: shear & peak



# WL peaks: A fast stochastic model

A fast stochastic model (See Lin & Kilbinger 2015a, A&A, 576, A24 for details)

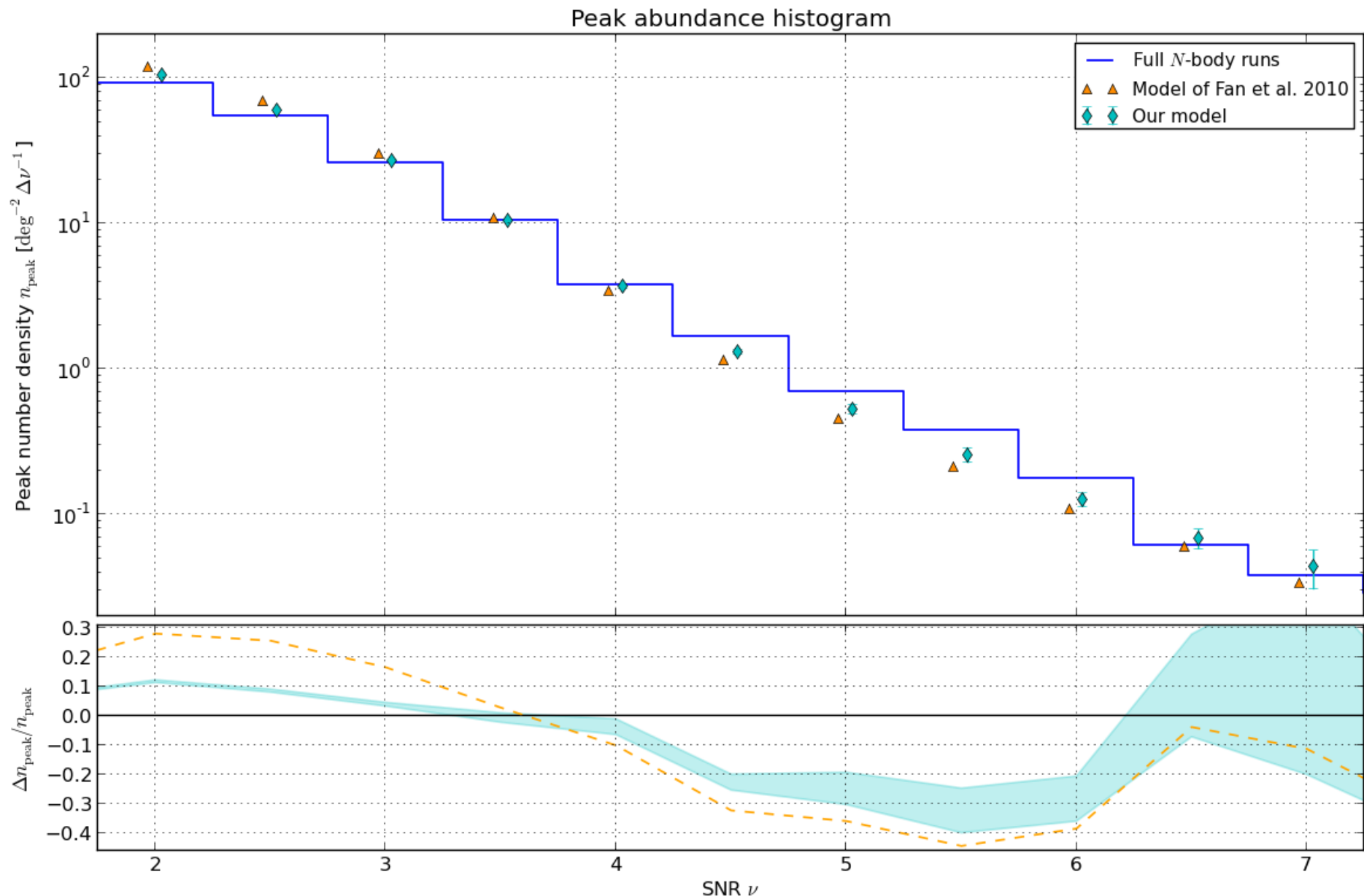
## Steps



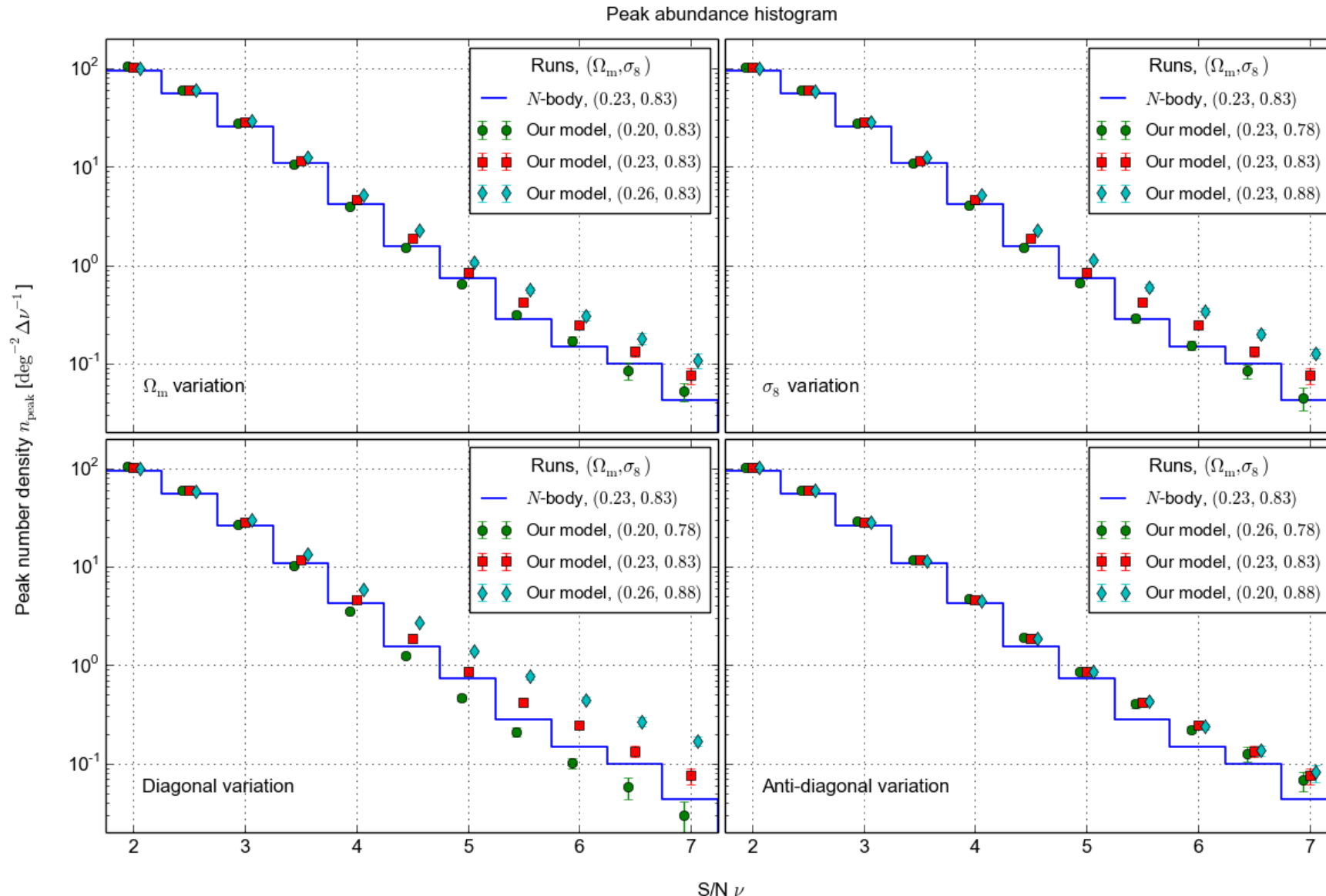
## Hypotheses

- Diffuse, unbound matter does not significantly contribute to peak counts
- Spatial correlation of halos has a minor influence

# WL peaks: histograms



# WL peaks: cosmological parameters



Lin &amp; Kilbinger (2015a)

# WL peaks: comment on stochasticity of model prediction

The camelus model for peak counts is stochastic: For given cosmological parameters, the model prediction is created from a random simulation process. Two model predictions for the same parameter will not be equal.

In fact, the scatter in a number of  $N$  model predictions reflects the sample variance and Poisson errors! Our model therefore does not only predict the mean but the full pdf of observables! (If scatter in our model is the true, underlying uncertainty.)

We do not need to assume an analytical functional form for the likelihood (e.g. Gaussian), do not need a covariance or its inverse.

We can use various general methods to obtain parameter constraints without limiting assumptions.

**Example:** ABC, Approximate Bayesian Computation (next slide).

# ABC: illustration of the principle

ABC's accept-reject process is actually a sampling under  $P_\epsilon$  (green curve):

$$P_\epsilon(\pi|x^{\text{obs}}) = A_\epsilon(\pi)P(\pi),$$

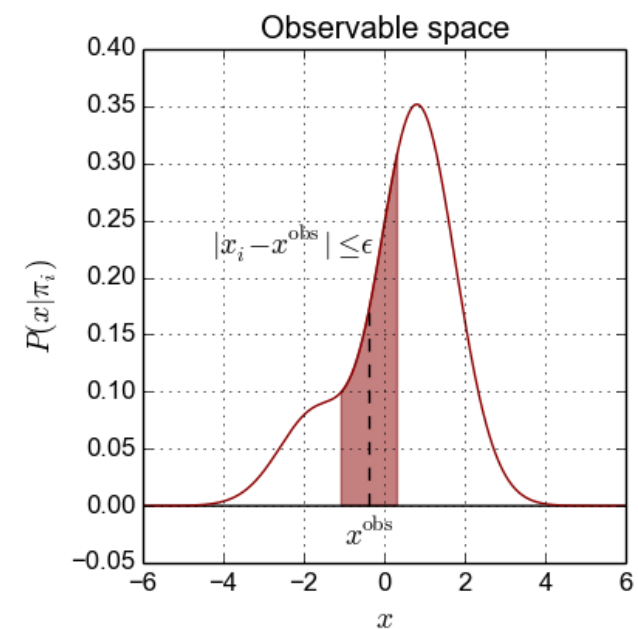
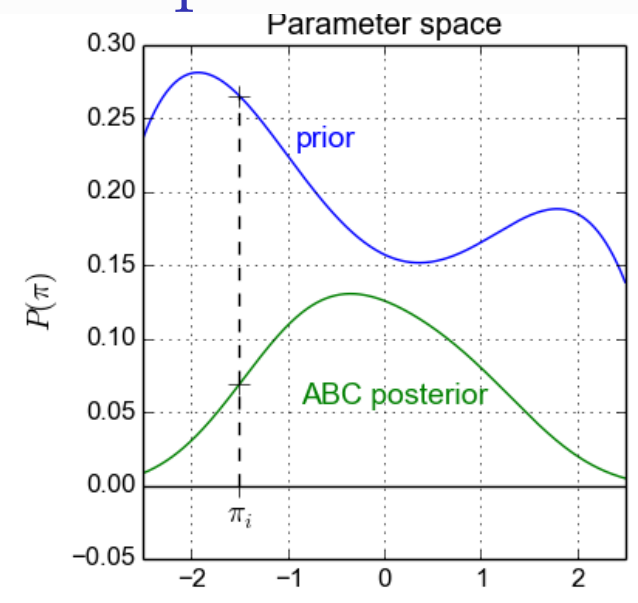
where  $P(\pi)$  stands for the prior (blue curve) and

$$A_\epsilon(\pi) \equiv \int dx P(x|\pi) \mathbb{1}_{|x-x^{\text{obs}}| \leq \epsilon}(x),$$

is the accept probability under  $\pi$  (red area). One can see that

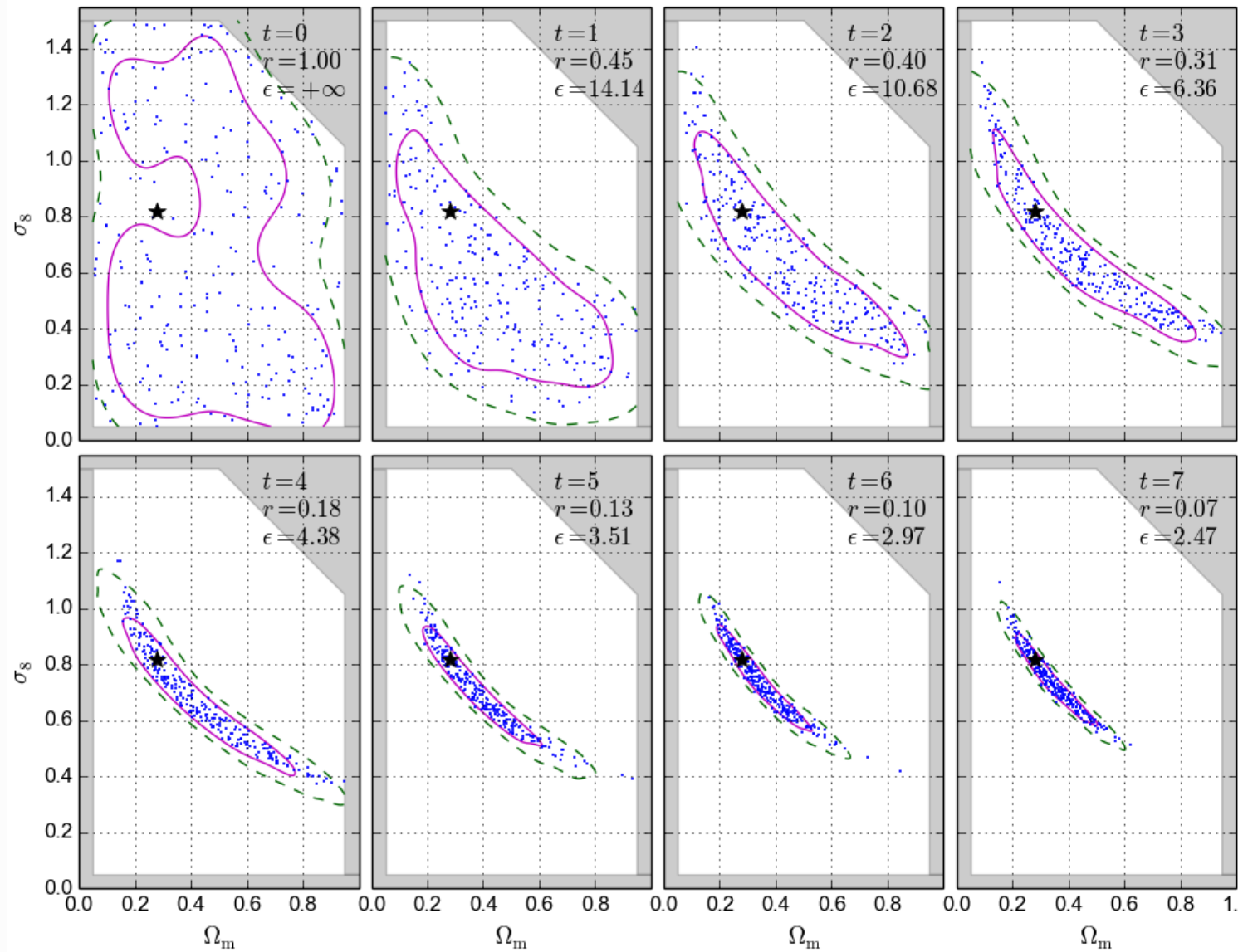
$$\lim_{\epsilon \rightarrow 0} A_\epsilon(\pi_0)/\epsilon = P(x^{\text{obs}}|\pi_0) = \mathcal{L}(\pi_0),$$

so  $P_\epsilon$  is proportional to the true posterior when  $\epsilon \rightarrow 0$ .



# WL peaks: ABC, results from simulations

PMC ABC posterior evolution



Lin &amp; Kilbinger (2015b)